

RIGA TECHNICAL UNIVERSITY
Faculty of Mechanical Engineering, Transport and Aeronautics

Sergejs BRATARČUKS
Student of the Doctoral study program “Transport”

**ASSESSMENT OF TECHNICAL CONDITION OF THE
LAND TRANSPORT STRUCTURES AND OBJECTS
USING ACOUSTIC EMISSION METHOD**

Summary of the Doctoral Thesis

Scientific Supervisor
Professor, *Dr. habil. sc. ing.*
M. BANOVS

RTU Press
Riga 2017

Bratarčuks S. Assessment of Technical Condition of the Land Transport Structures and Objects Using Acoustic Emission Method. Summary of the Doctoral Thesis. – Riga: RTU Press, 2017. – 41 p.

Printed according to the decision of the RTU P-22 Board meeting, November 10, 2016, Protocol No. 05/2016

DOCTORAL THESIS
PROPOSED TO RIGA TECHNICAL UNIVERSITY FOR THE
PROMOTION TO THE SCIENTIFIC DEGREE OF DOCTOR OF
ENGINEERING SCIENCES

To be granted the scientific degree of Doctor of Engineering Sciences (Transport), the present Doctoral Thesis has been submitted for the defence at the open meeting of RTU Promotion Council “RTU P-22” at RTU Aeronautics institute 1A k-1 Lomonosova Street, Riga, at 14:30 on 2017, September 14th, auditorium 218.

OFFICIAL REVIEWERS

Professor *Dr. habil. sc. ing.* Andrey Shaniavski
Material Research Division of Aviaregister, Russia

Professor *Dr. habil. sc. ing.* Valdis Priednieks
Latvian Maritime Academy

Assoc. Professor *Dr. sc. ing.* Margarita Urbaha
Riga Technical University

DECLARATION OF ACADEMIC INTEGRITY

I hereby declare that the Doctoral Thesis submitted for the review to Riga Technical University for the promotion to the scientific degree of Doctor of Engineering Sciences (Telecommunications) is my own. I confirm that this Doctoral Thesis had not been submitted to any other university for the promotion to a scientific degree.

Sergejs Bratarčuks(Signature)

Date:.....

The Doctoral Thesis has been written in English language; it consists of an introduction, five sections, conclusions, bibliography, and 10 appendices. It includes 91 figure and 10 tables. The total volume of the Thesis is 200 pages. The bibliography comprises 161 entry.

1. TABLE OF CONTENTS

GENERAL DESCRIPTION OF THE THESIS.....	6
CHAPTER 1: THE ANALYSIS OF METHODS FOR ASSESSING THE TECHNICAL CONDITION OF THE LAND TRANSPORT SYSTEMS' STRUCTURES.....	10
CHAPTER 2: THE METHODOLOGY OF EXPERIMENTAL AE-EXAMINATION OF DAMAGES OF LAND TRANSPORT CONSTRUCTIONS	11
2.1 The objects of technical condition assessment	11
2.1.1 Çegums HPP bridge.....	11
2.1.2 Locomotive bogie frames and bolsters	12
2.1.3 Prestressed concrete railway sleepers	13
2.2 The test objectives.....	13
2.3 AE registration and measurement equipment	14
2.4 Çegums HPP bridge inspection methodology	15
2.5 The methodology of assessment of 2M62 locomotive bogie frames and bolsters	15
2.6 The methodology of AE testing of prestressed concrete sleepers	18
CHAPTER 3: EXPERIMENTAL STUDIES OF THE MECHANISMS OF DAMAGE TO LAND TRANSPORT FACILITIES AND THE EVALUATION OF THE TECHNICAL STATE BY THE METHOD OF ACOUSTIC EMISSION.....	19
3.1 Application of AE in the assessment of Çegums HPP bridge	20
3.2 Assessment of the 2M62 locomotive bogie frames and bolsters	20
3.3 Features of behavior of AE signals at dynamic bench tests of prestressed concrete sleepers	21
CHAPTER 4: INVESTIGATION OF DAMAGES OF MODERN COMPOSITE MATERIALS AND DEVELOPMENT OF ASSESSMENT CRITERIA USING THE SPECTRAL PROPERTIES OF AE-SIGNALS.....	26
4.1 Description of the subject area.....	26
4.2 Material characteristics	27
4.3 Research objectives.....	27
4.4 Test methods	27
4.5 Test results	30
4.6 Chapter summary	31
CHAPTER 5: MATHEMATICAL ANALYSIS OF SPECTRAL AND DYNAMIC CHARACTERISTICS OF AE-SIGNALS AND DEVELOPMENT OF A MATHEMATICAL METHOD FOR IDENTIFYING THE STAGES OF MATERIAL DESTRUCTION.....	31
5.1 Problem description	31
5.2 The problem of compatibility of AE systems	31
5.3 Data normalization function.....	31
5.4 Determination of dynamic α_1 и α_2 criteria using the “smoothing” function.....	32
5.5 Development of the program AE frequency analysis	33
5.6 Determination of the maximum frequency power spectrum density	34
5.7 Determination of α -criterion connection with the spectral characteristics of AE signals during destruction of epoxy composite.....	35

5.8 Method verification..... 38
CONCLUSIONS..... 39
BIBLIOGRAPHY 40

GENERAL DESCRIPTION OF THE THESIS

Research topicality

Transport is one of the most important sectors of the economy, shaping and defining the opportunities for the development of all other areas of the activity of the modern countries. The constantly increasing demand for more intense, high-speed ground transportation systems results in the use of all elements of the transport infrastructure with increasing loads. The wheels of locomotives, wagons, and axle trucks are subject to the complex effects of fatigue loads, shock loads, and other impacts.

In January 2014, a new policy was adopted by the EU on the development of transport infrastructure. This policy is related to the gradual deployment of the transport infrastructure projects of TEN-T (Trans-European Transport Networks), which began in the early 1990s. The planned date of the implementation of the project is year 2030, with 24.05 bn. € of the draft budget to be spent until 2020 [7]. The task of the group of projects TEN-T is to improve the opportunities for economic growth and bring together the individual European national transport networks. The result would be the expansion of the transportation capacity, the creation of new transport links, and the modernization of existing ones. For Latvia, as for the European Union member, participation in TEN-T is an important and topical task. Among the 30 priority projects, there is the draft “PR 27 Rail Baltica”, which directly affects Latvia. There will be high-speed sections of the railway on which traffic will be much more intensive than on the Latvian railways at the moment.

The growth of rail traffic and the changes in the direction of the movement of cargo tend to inevitably lead to the changes in other modes of transport. The result is the demand for new roads and driveways. At the same time, a more thorough assessment of the resource overpasses, bridges, dams, mode of use has been less intense is required. This means that the improvement of diagnostic methods and the control of the elements of the transport infrastructure and rolling stock will be needed.

One of techniques that allows diagnosing the accumulation and development of damages in infrastructure projects, units and aggregates of machines, in tanks, pipes or any other objects, is the acoustic emission method (AE). This method belongs to the family of non-destructive testing methods (NDT). The method is based on the principle of the recording and decoding of high-frequency acoustic signals that emit developing defects in materials under the influence of stress. The important circumstance is the fact that the load-AE while monitoring may be used within the normal operating loads, which allows assessing the state of an object without sacrificing it.

The topicality of this study is due to the ever-growing demand of the economy to ensure transport safety in load growth in the transport network. The work is devoted to the use and development of the method of the non-destructive testing of materials, components and ground transportation systems based on the acoustic emission phenomenon.

Aim and objectives of the research

Aim

Carry out a study of the mechanics of damaging materials and structures, and develop a multicriteria methodology for the acoustic emission testing for assessing the technical condition of land transportation facilities.

Objectives

1. Conduct a comparative analysis of the traditional methods of nondestructive testing and the AE method and substantiate the possibility of using AE parameters for solving the problem of assessing the transport objects.
2. Carry out an experimental study of the mechanisms of damage to land transport facilities, and determine the AE criteria for assessing their technical condition.
3. Determine criteria for assessing the damage of modern composite materials, using the spectral properties of AE signals.

4. Conduct a mathematical analysis of the spectral and dynamic characteristics of AE signals and develop a mathematical method for identifying the stage of material destruction.
5. Develop a multi-criteria methodology for AE testing to assess the technical condition of ground transportation facilities in operation.
6. Based on the obtained spectral and dynamic characteristics of AE signals, develop software for AE analysis, and perform a check of its functions in the process of assessing the technical condition of the objects under study.

Research methods

1. Analysis of literature.
2. Comparative methods.
3. Empirical experimental methods.
4. Mathematical analysis.
5. Mathematical programming.

Objects of study

1. Kegums Hydro Power Plant bridge over the Daugava river driving section bearing beams.
2. 2M62 locomotive bogie frames and bolsters
3. Reinforced concrete railway sleepers.
4. Epoxy PES-filled composite samples.

Scientific novelty and the key innovations of study

The scientific novelty of the thesis is as follows:

- 1) a multiparametric method for analyzing the properties of AE signals has been developed, which makes it possible to assess the technical state of the objects and structures of land transport;
- 2) the nature of the correspondence of the stages of the fracture of composite materials to the combined AE parameter is determined, which includes the rate of the growth of the total AE and the maximum spectral density of the AE;
- 3) a new cross-platform software has been developed that allows analyzing the changes in the intensity of AE, the second derivative of intensity, the spectral properties of AE together with the parameters of the testing machine, and also assessing the degree of the mutual correspondence of AE patterns. This makes it possible to improve the informative value of the AE method and more efficiently conduct AE experiments.

The practical importance of the Thesis

Developed innovative solutions have been used in assessing the technical state of the bridge crossing of the Kegums Hydroelectric Power Plant (HPP), elements of the locomotive, pre-stressed concrete sleepers, and also for testing modern composite materials. The results of the present Doctoral Thesis have practical significance, since the research has developed both a new method for determining the stages of destruction and an instrument for data analysis that allows these methods to be implemented. The results of the Thesis open new possibilities for the comprehensive application of the AE method in checking the technical condition of the objects and devices used in land transport.

Approbation of the obtained results

The main scientific and practical results of the work have been presented at eight scientific conferences

1. The 9th International Conference on Information Technologies and Management 2011, Bratarchuk S, Sazonovs A, *Approaches for obtaining and Processing Snow Avalanche Acoustics Emission Data*. – April 14–15, 2011, Riga, Latvia

2. Research and Academic Conference Research and Technology – Step into the Future, Urbahs A, Banov M, Turko V, Bratarchuk S, Khodos N, Feshchuks J, *Features of Behaviour of Acoustic Emission Signals at Dynamic Tests of pre-stressed concrete elements of railways*. – December 10–11, 2010, Riga, Latvia
3. Riga Technical University 52nd International Scientific Conference, Urbahs A, Banovs M, Bratarčuks S, *Indication and Prediction of the Landslides Occurrence Process Based on the Acoustic Emission Method*. – October 13–16, 2011, Riga, Latvia
4. Riga Technical University 51st International Scientific Conference, Urbahs A, Banovs M, Harbuz Y, Bratarčuks S, Khodos N, *The Applicability of the acoustic emission method to check the mill rolls*. – October 11–15, 2010, Riga, Latvia
5. Intelligent Transport Systems (ITS'12), Bratarchuk S, *Investigation of the weak vibrations effect on the deformation of rocks by the acoustic emission method*. – July 18–20, 2012, Riga, Latvia
6. Intelligent Transport Systems (ITS'12), Urbahs A, Banov M, Bratarchuk S, Khodos N, Serebrjakovs P, Turko V, *Diagnostics of aircraft elevator's skin zones after the impact of lightning using the method of acoustic emission*. – July 18–20, 2012, Riga, Latvia
7. Riga Technical University 53rd International Scientific Conference dedicated to the 150th Anniversary and the 1st Congress of World Engineers and Riga Politechnical Institute / RTU alumni, Urbahs A, Banov M, Bratarchuk S, Khodos N, Serebrjakovs P, Turko V, *Diagnostics Of 7-Layer Composite Materials After The Impact Of Lightning Using The Method Of Acoustic Emission*, October 11–12, 2012, Riga, Latvia
8. Riga Technical University 57th International Scientific Conference, Bratarchuk S, *Ways of improving methods of collecting and interpreting AE data*, October 14-15, 2016, Riga, Latvia

Publications

The results have been published in seven papers

1. Bratarchuk, S.
Indication of stage of destruction of epoxy PES-filled composite using connected parameter of acoustic emission rate and the spectral characteristics of AE signals.
Submitted to: Transport and Aerospace Engineering, Vol. 4, Iss. 1, 2017.
ISSN 2255-9876
2. Bratarchuk, S.
Assessment of technical condition of 2M62 locomotive bogie frames and bolsters using acoustic emission method.
Submitted to: International Conference “Mechanika-2017” Proceedings, Lithuania.
3. Urbahs, A., Banovs, M., Bratarčuks, S., Serebrjakovs, P., Turko, V.
Diagnostics of Damaged Composite Skin Zones of Aircraft after the Impact of Lightning Bolt Using the Method of Acoustic Emission.
From: Proceedings of the 16th European Conference on Composite Materials (ECCM 2014), Spain, Seville, June 22–26, 2014. Seville: 2014, pages 1–8.
4. Bratarčuks, S., Dubovska, R.
Using Car Vibration Data for Road Prominency Identification.
From: Information Technologies, Management and Society: The 12th International Scientific Conference “Information Technologies and Management”, Latvia, Riga, April 16–17, 2014. Riga: ISMA University of Applied Sciences, 2014, pages 36–37. ISSN 1691-2489
5. Bratarčuks, S., Sazonovs, A.
Approaches for Obtaining and Processing Snow Avalanche Acoustics Emission Data.
From: Information Technologies, Management and Society: The 9th International Conference on Information Technologies and Management, Latvia, Riga, April 14–15, 2011.

Riga: Information Systems Management Institute, 2011, pages 63–63.

ISSN 1691-2489

6. Urbahs, A., Banov, M., Turko, V., Bratarčuks, S., Khodos, N.
Some Features of Behaviour of Acoustic Emission Signals at Dynamic Bench Test of Prestressed Concrete Sleepers.
From: Proceedings of the 14th International Conference “Transport Means 2010”, Lithuania, Kaunas, October 21–22, 2010. Kaunas: Technologija, 2010, pages 45–48.
7. Urbahs, A., Banovs, M., Turko, V., Bratarčuks, S., Khodos, N., Feščuks, J.
Features of Behavior of Acoustic Emission Signals at Dynamic Tests of Prestressed Concrete Elements of Rail Ways.
From: Research and Technology – Step into the Future, Vol. 5, No. 3, Latvia, Riga, December 10 – January 11, 2010. Riga: Transport and telecommunication institute, 2010, pages 106–106.

Structure of the Thesis

The Doctoral Thesis consists of an introduction, five chapters, results and conclusions, a bibliography, and 10 appendices. It is illustrated by 91 figure and 10 tables. The total volume of the present Thesis is 200 pages. The bibliography contains 161 entry.

SUMMARY OF THESIS CHAPTERS

CHAPTER 1: THE ANALYSIS OF THE METHODS FOR ASSESSING THE TECHNICAL CONDITION OF THE LAND TRANSPORT SYSTEMS' STRUCTURES

Non-destructive testing methods (NDT) play an important role in the system of transport services and transport infrastructure because they provide early detection of internal defects in objects. One of the objectives of these methods is the detection of potentially dangerous defects, which can lead to accidental damage to the object in the future. AE method belongs to the family of non-destructive testing methods and is used to detect defects in the early stages of their development. Nowadays, acoustic emission testing has become a widely used method of non-destructive testing. AE method covers the characteristics of the signal, taking into account the place of their origin, stress intensity, and frequency characteristics [10].

The main difference of the acoustic emission method of the non-destructive testing of other NDT methods is the passive nature of the AE method (Fig. 1.1).

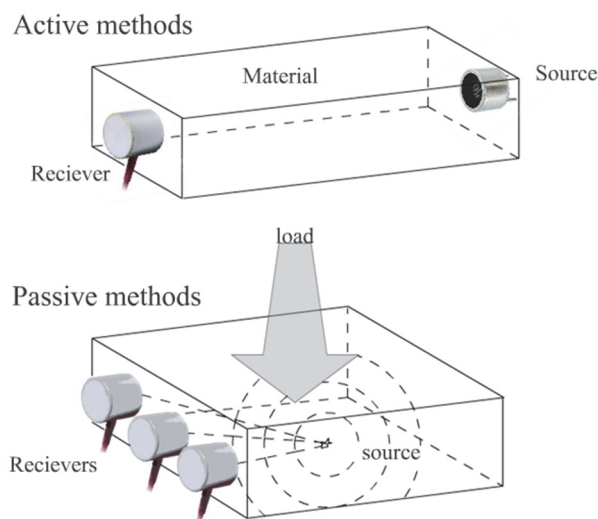


Fig. 1.1. Active and passive methods of ultrasound studies.

The unique properties of the AE method, making it the preferred method in the monitoring of the objects of transport and transport infrastructure, led to the spread of its use. The advent of high-speed computing, improvement of mass storage devices allows effective using of the method in assessing the condition of the objects and predict the durability in all types of ground transportation.

In the area of road transport, AE method is used in the research of materials, individual machinery units and mechanisms, as well as large engineering structures. Among the listed, tunnels, arched bridges, concrete and steel road structures, and prestressed reinforced concrete structures can be mentioned [3], [19]. One relatively new AE application related to road transport is the testing of the underwater concrete structures. The AE testing of underwater bridge supports can detect the fatigue defects in the conditions that make it impossible to use other NDT methods [11].

Pipelines often lie under the earth, and to determine the exact location of the leak is very important for the organization of repair due to the difficulty of access to the object [1]. Acoustic emission studies not only allow one to work with an already existing pipeline breach of integrity but also to detect the beginning of the mechanical and corrosive destruction for the purpose of accident prevention and the timely correction of defects [24].

In rail transport, AE method makes it possible to detect the defects in steel bridges [9] and in the structure of the rail [25]. The methods of application of AE as a monitoring tool to assist in real-time to determine the occurrence of defects in the bearings on the shaft of the wheelset are developed [2], [14], [20]. AE helps identify the structural degradation in alloys, which are shell construction materials of the gearboxes of high-speed trains.

In the area of rail transport, a new generation of AE method is used to assess the condition of superconducting magnets in train suspension systems using the method of magnetic levitation (maglev). AE helps detect the magnets emerged from the state of superconductivity and returned to the normal resistive state [12]. Application of AE method to solve the problem of defective magnet localization is not invasive and does not require disassembly of the entire structure. Based on a critical analysis of the current state of the periodic AE control, the conclusion that the methods for recording the moment of the occurrence of fatigue cracks are valuable in terms of operational control, but it is difficult to implement them to the specific objects of transport. There is a need in the description and in the improvement of the methods for determining α -test, as well as in the identification of additional settings of AE, which can carry information about the stage of destruction. The development of the methods of collecting and processing the acoustic emission data, a description of the destruction of the models of different materials and transport facilities, is an important work in the field of non-destructive testing methods.

In the first chapter, the variety of the use of NDT methods in land transportation is shown. The AE method is specially emphasized, because it is considered a passive testing method, which means its usage is based on such signals that only occurred in the object due to its exploitation.

The AE method plays an important role in the family of other NDT methods. In some cases, the application of the AE method is the only way to determine the technical state of an object. This unique method has both physical advantages in applying to various objects (testing of underwater concrete structures etc.), and economic advantages (limitation of testing time and costs). There are also cases when it is required to use all possible methods of nondestructive testing to verify the same object in order to guarantee the quality of the technical evaluation.

The need for non-destructive monitoring of objects during operation is associated with the task of preventing the destruction of the control systems and structural elements of transport facilities. The application of AE improves the possibilities of early detection and localization of defects.

Based on a critical analysis of the current state of AE control, it is concluded that methods for detecting the fatigue damage during operation are valuable for monitoring the state of objects, but are often difficult to apply. There is a need to develop and improve the interpretation of dynamic criteria for AE signals, as well as to apply other parameters of AE signals that carry information about the stage of destruction. The development of the methods for collecting and processing the AE data as well as the description of destruction models for various new materials, and pattern processing techniques [23] is an actual and necessary work in the field of non-destructive testing methods.

CHAPTER 2: THE METHODOLOGY OF EXPERIMENTAL AE EXAMINATION OF THE DAMAGES OF LAND TRANSPORT CONSTRUCTIONS

2.1 The objects of technical condition assessment

2.1.1 Ķegums HPP bridge

The keeping of dangerous technical facilities such as bridges in the normal technical condition is a priority for the organizations operating these facilities. Hazardous industrial facilities are included in the class of dangerous equipment that in the law of the Republic of Latvia “On technical supervision of dangerous equipment” is formulated as follows: dangerous equipment – machines and equipment systems that could threaten human life and health, environment and material values [5]. In the second chapter, the characteristics of the assessment of the technical state of Ķegums HPP bridge as well as the description of AE hardware and testing methodology are given. The object of the research is the bridge crossing that serves for the movement of road transport that is a three-span section of different lengths (Fig. 2.1).

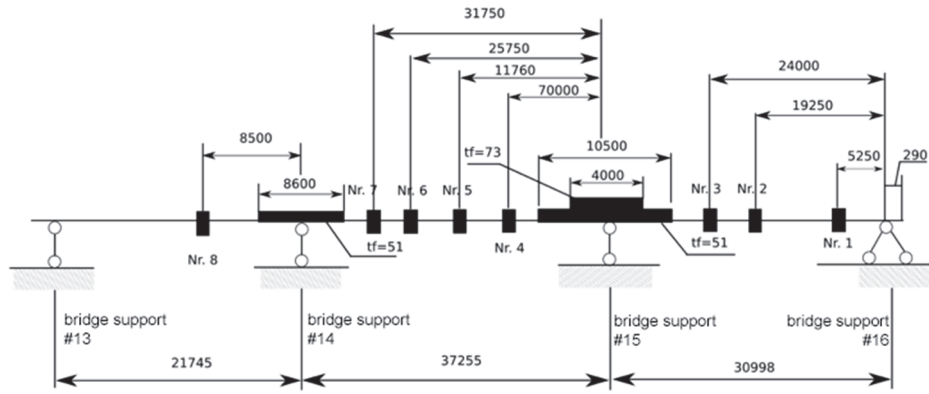


Fig. 2.1. The scheme of the Kegums HPP bridge.

The basis of the driving section is two-bearing I-section beams, consisting of the left and right sides, connected to bridge supports. The pavement is laid on the basis (Fig. 2.1). Each beam is assembled from two similar parts, which are interconnected back to back (Fig. 2.2). Every joint on both sides has eight pads as indicated in Fig. 2.2 – digits 1, 2... 8. Cover plates connect the adjacent ends of the adjacent pieces of beams using the rivets.

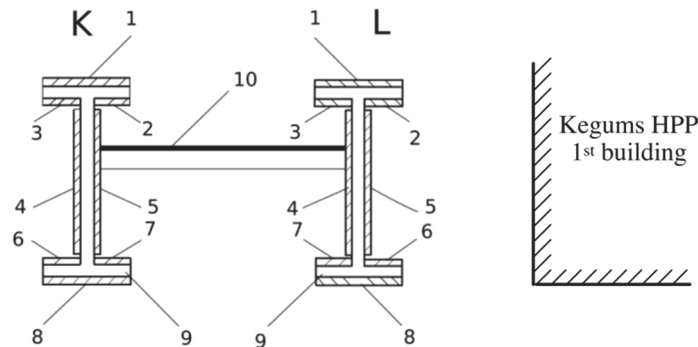


Fig. 2.2. Driving section bearing bridge beams (K – left side; L – right side).

The elements indicated in Fig. 2.2 are as follows: 1 – top pads; 2 – right lower lining at the top of the beam; 3 – left lower trim at the top of the beams; 4 – left-side plates; 5 – right-side plates; 6 – upper right pad at the bottom of the beam; 7 – covers the upper left-bottom of the beam, the lower-pad; 8, 9 – bearing beams; 10 – the road surface.

2.1.2 Locomotive bogie frames and bolsters

The basic elements of locomotives and freight cars casted elements work in the critical conditions of the influence of dynamic and static loads. This is especially true of such elements as the bogie frame, bolster, and side frame axle bogies. The destruction of these elements can lead to dangerous consequences for people, the environment, and infrastructure. The problem of the fracture of cast parts bogie is not new to the rail transport.

Characteristics of the objects of study

1. Carriage number 166 (the year of manufacturing – 1982): total mileage from the time of manufacture – 1,516,761 km. Renovated TR-3 (current repair), the term of bogie service was extended until April 2021 (Fig. 2.3.).
2. Carriage number 184 (the year of manufacturing – 1970): total mileage from the time of manufacture – 1,149,520 km. Renovated TR-3 (current repair), bogie service life has been extended until April 2015 (before write-off).

Note. The deadline for service of the locomotive 2M62 and its trucks is defined 45 years.

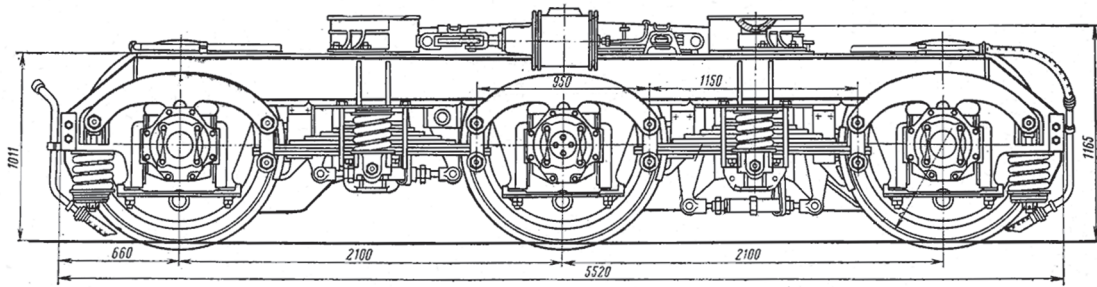


Fig. 2.3. Side view of a trolley locomotive M62 assembly [13].

2.1.3 Prestressed concrete railway sleepers

The object of study – the most used in Latvia concrete sleepers. These are prestressed concrete beams, reinforced by high tensile steel wire bars with a diameter of 3.14 mm (Fig. 2.4). The nominal number of wires in a tie of a tested sleeper: 44.

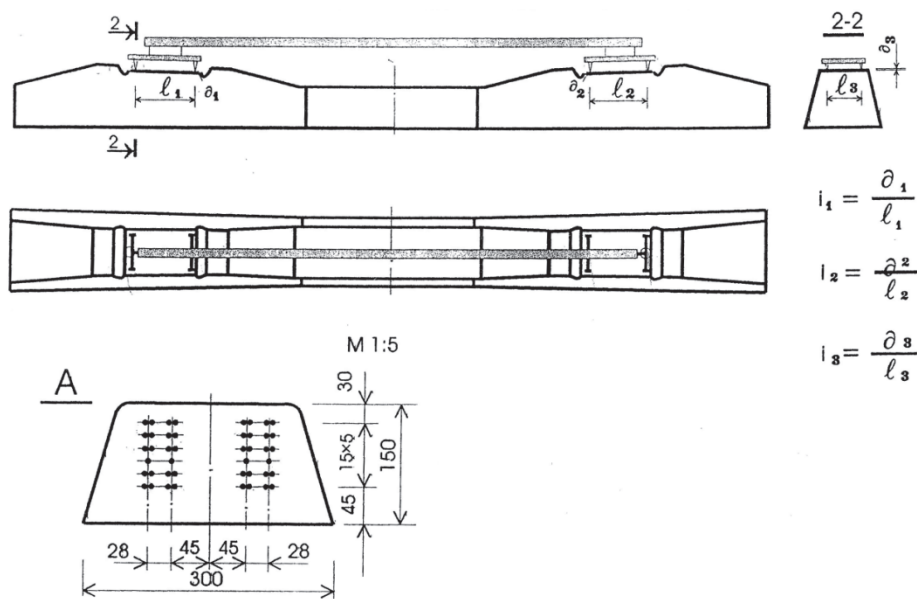


Fig. 2.6. Drawing of the tested sleeper.

Each of wires is stretched with a force of 8,1 kN. Thus, the total load of a sleeper's ties after hardening of concrete reaches 356,4 kN. The main defects of concrete sleepers are:

- 1) transverse cracks in rail pad position,
- 2) fracture of the sleepers in the rail area,
- 3) transverse cracks in the middle of the sleeper,
- 4) the breaks in the middle of the sleeper,;
- 5) longitudinal cracks passing through the holes for bolts embedded,
- 6) chips of concrete sleepers.

The causes of these defects depend on the manufacturing quality of concrete sleepers and are determined mainly at operating conditions.

2.2 The test objectives

Ķegums HPP bridge

1. Identification of the most defective pads in each junction.
2. Evaluation of the corrosion of the wear linings of joints bearing the beams of the bridge.
3. Evaluation of the corrosion and deterioration of riveted joints.

4. Assessment of the impact of the corrosion deterioration of compounds on their load-bearing capacity.

Note: the first objective was achieved with random loading of the bridge, the second and the third objectives were achieved using artificial AE signals, and the fourth objective was achieved through the creation of a test load on the bridge.

Locomotive bogie frames and bolsters

1. Assess the current technical condition of the bogie frames 2M62 freight locomotives and bolsters of two-axle bogies.
2. Identify the need for other methods of non-destructive testing by assessing the state of the objects of research by AE.
3. Extend the assigned service life of locomotive bogie frames.
4. In cast constructions of bogies wagons with a resource that cannot extend: check the quality of the factory production technology and compare it with the design strength calculation.
5. Check the nature of the AE occurrence of alpha-test during fatigue tests.

Prestressed concrete railway sleepers

1. Quantify the breaking load in the prestressed concrete sleepers.
2. Identify the features of exhibiting α -criterion and identify the opportunities for its use for the assessment of concrete sleepers.
3. Identify the mechanisms that determine the character of the appearance of acoustic emission in the tested object.

2.3 AE registration and measurement equipment

AE equipment used for testing Kegums HPP bridge

1. PAC 3000/3104 system (bandwidth of 20 kHz – 2 MHz) (Fig. 2.7).
2. Calibrator AECAL-2.
3. A kit based on two AF-15s.
4. Preamplifiers.
5. AE sensors.

AE equipment used for testing the 2M62 locomotive bogie frames and bolsters

1. The unit of acoustic emission registration: Lel/A-Line 32D (DDM)/-DIGITAL acoustic emission system A-Line 32D (Fig. 2.8.). This is multichannel modular system of AE data acquisition and processing with a high-speed digital serial data link.
2. Acoustic emission transducers: acoustic emission GT200 resonance-type converters with the operating frequency of 165 kHz and the bandwidth of 130–200 kHz were used.

AE equipment used for testing the prestressed concrete railway sleepers

1. PAC 3000/3104 system (bandwidth of 20 kHz – 2 MHz).
2. Preamplifiers.
3. Physical Acoustics Pocket AE acoustic emission portable computer with built-in 26 dB preamplifiers (Fig. 2.9).
4. P-113 (0.02–0.2 MHz) piezo AE sensors.

2.4 Ķegums HPP bridge inspection methodology

Random loading was created with normal movement of vehicles on the bridge. The measurement and registration of AE signals were carried out in the joints No. 1 and No. 8 with the PAC 3000/3104 AE measuring kit.

It was revealed that the most “noisy” and, hence, the loaded (worn, defective) joints are the place of the lower connection of pads 6, 7, and 8 (see Fig. 2.2) with bearing beams. The evaluation of the corrosion deterioration of the joint parts of the bridge was carried out by measuring the acoustic emission characteristics of the path between the two joined parts with the test of AE signal, which is used as one of the AE sensors. One of AE sensors was used as an ultrasonic emitter (a pulsar). The pulsar sensor was housed in one of the joint connected parts. Signals were registered using AE sensor, respectively, at opposite connection parts (Fig. 2.5). The signal control was carried out using the AE PAC3000/3104 device. The methodology refers to the patent of Latvia No. Cl.:G01N29/14 [21].

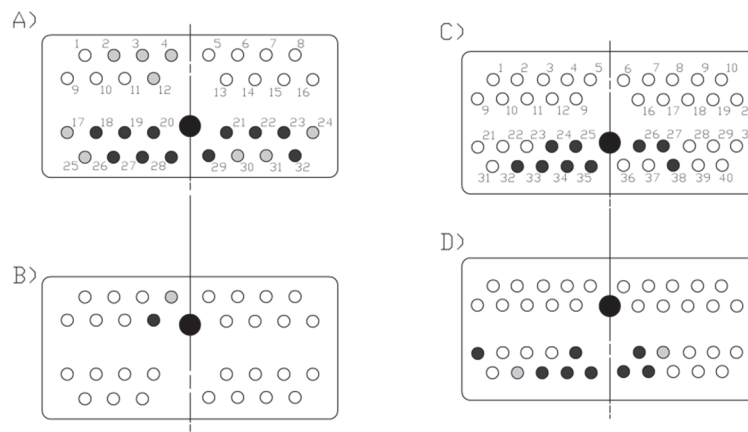


Fig. 2.5. Scheme of the rivets numbering and the test results on the bottom of the joints No. 3 and No. 6.

In order to evaluate the corrosion wear on the bearing capacity of the joint produced loading bridge load test, which served as a truck of the total weight of five tons, moving on the bridge at a speed of 16 m/s. Comparative assessment was applied to the joints No. 3 and No. 6, which degree of corrosion damage was revealed in the previous step.

2.5 The methodology of the assessment of the 2M62 locomotive bogie frames and bolsters

Tests were conducted in two stages.

Stage 1 – static loading carts frames in the conditions of bench tests and in the conditions of the locomotive depot.

Stage 2 – dynamic testing of bogie frames and bolsters to assess their survivability since the emergence of the fatigue crack prior to their destruction.

Test programs on the stand and on the locomotive were selected identically. The difference was in the extreme force: on the stand, it exceeded the maximum operating weight of the body of the locomotive, i.e., 10%. The locomotive is fitted to the depot to four power jacks. Measured compression springs with the full weight of a 100 % workload. For data collection, GT-200 AE piezoelectric transducers of A-Line system 32 DDM were arranged in such way: three sensors on a trolley, along the outer edge of the top sheet of the lateral beam of bogie frames according to the scheme shown in Fig. 2.6. The sensors and modules of the system were mounted (Figs 2.7 and 2.8).

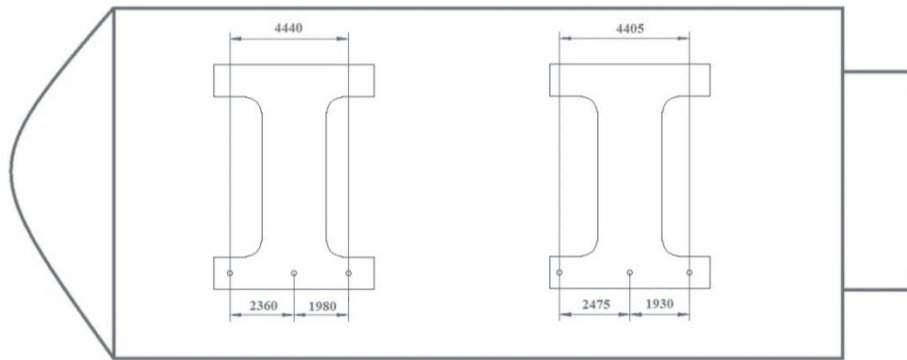


Fig. 2.6. The alignment of LeI/A-Line 32 DDM control system sensors on the locomotive bogies frames.



Fig. 2.7. The alignment of AE control system modules on the locomotive bogie frames.



Fig. 2.8. Control sensors attachment on the bogie frame of the locomotive.

The whole system of six modules was connected in a line. The initial discrimination thresholds were set at 35dB. Further, the calibration was performed by the method of Su-Nielsen (breaking of a graphite pencil lead with the diameter of 0.5 mm and hardness of HB) to select the gain [22]. As a result of the calibration, the coefficients of gain modules were set at 40 dB. Locomotive body was lifted up to complete the unloading of trucks and the spring compression at zero load was measured. Compression was measured at 25% of the workload. Next, it was switched on the A-Line 32 DDM AE system and produced a cyclic loading body of carts by the weight of the locomotive on the program shown in Fig. 2.9.

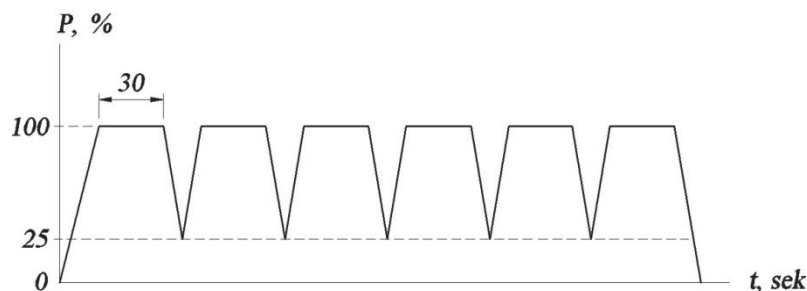


Fig. 2.9. The program of statically repeated loading.

With an operating time of approximately 5×10^6 cycles, when the fatigue crack has not yet been noticed visually, the bogie frame test structure was modified through a step-by-step introduction of the cut concentrator in one of the power units of the frame supports. It was made for the early appearance of a fatigue crack.

It can be seen in Fig. 2.10 that when the stand being operational during the 1100–1200 seconds with initially introduced cuts, the AE intensity began to grow sharply, pointing out that there began to form fatigue cracks in the area of the 2nd sensor near the concentrators. In this mode, the test lasted for 80 000 seconds more. But a periodic visual inspection did not find anything similar to the appearance of fatigue cracks. However, when the cumulative AE graph was identified with the fracture failure morphology, it was found that the moment α_1 of cumulative AE steep rise corresponds to the appearance of fatigue cracks, and the moment α_2 corresponds to the early emergence and growth of macrocracks.

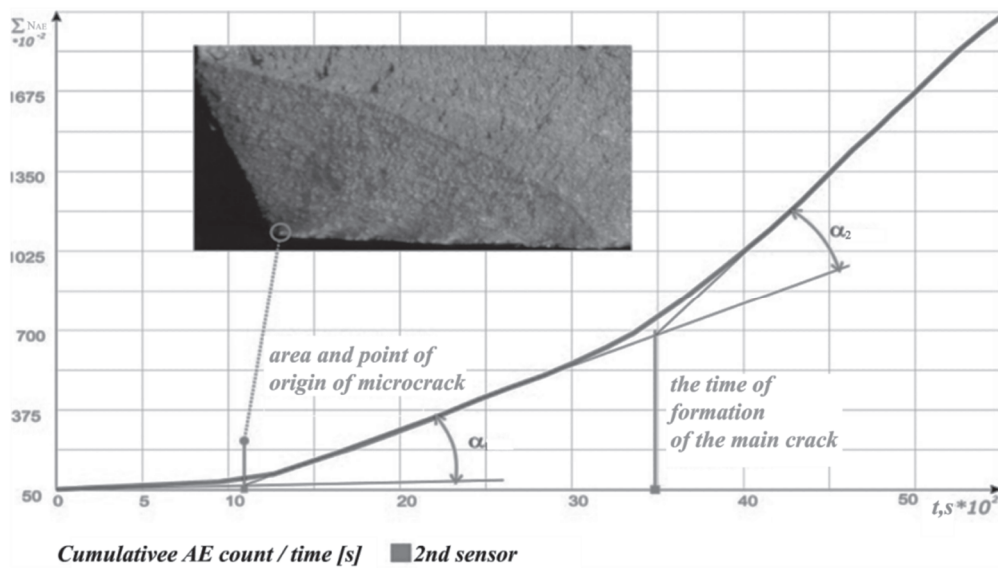


Fig. 2.10. The dependence of the amount of AE on loading from the moment of the first group of hubs and the morphology of the fracture at this point.

The test program was the same as for the bogies frame. Bolster was tested under the three-point variable cyclic-bending constant-sign scheme with the frequency of the load 8 Hz, amplitude $\Delta P = 12.5$ t. AE sensor attachment scheme is shown in Fig. 2.11.

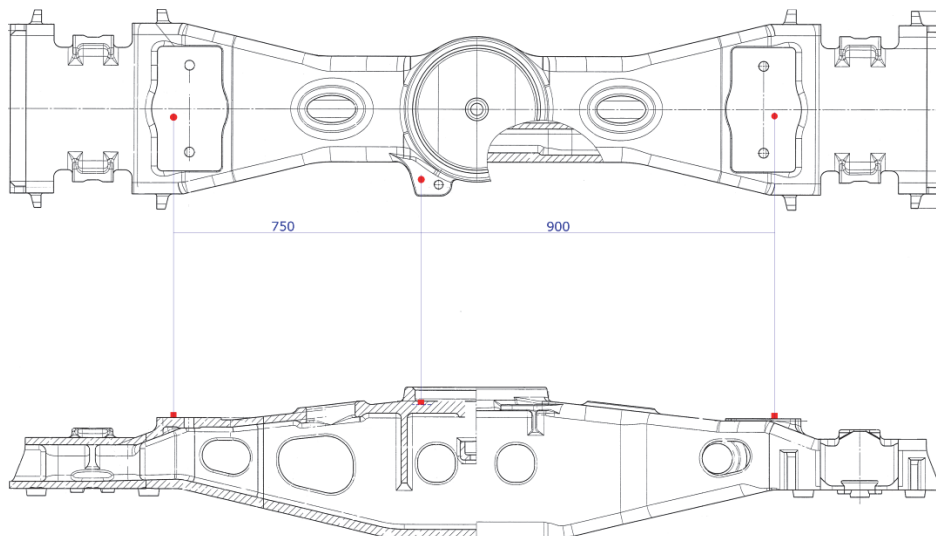


Fig. 2.11. The plan for the AE sensors.

2.6 The methodology of AE testing of prestressed concrete sleepers

Operating loads are cyclic loads of constant sign in the areas under the rail foot from impinging wheelsets. Therefore, the quality control of manufacturing technology sleepers was conducted using the fatigue test according to the scheme of single beam sleeper loading (Fig. 2.12).

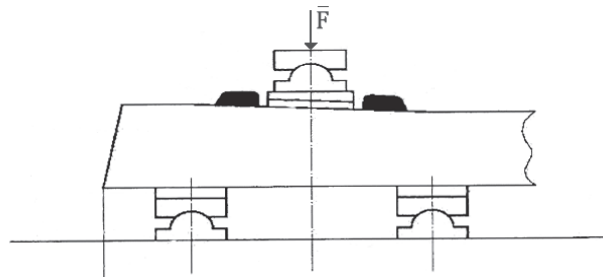


Fig. 2.12. Scheme of dynamic loading of monobloc sleepers' full load.

Thus a typical amplitude variation within a load cycle is close to sinusoidal (Fig. 2.13).

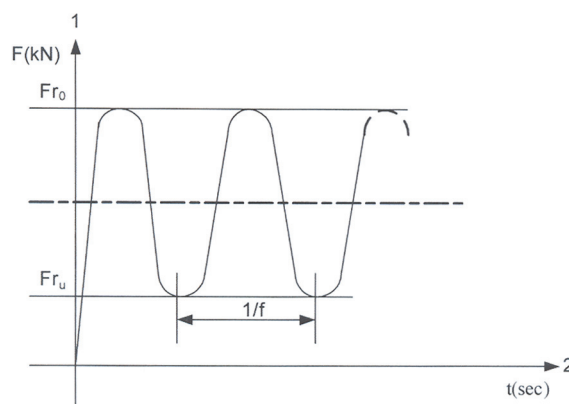


Fig. 2.13. Graph of the changes in loading amplitude in fatigue tests.

The remaining steps for determining the variable load limit at which the sleeper is destroyed are provided in accordance with [6] the application of dynamic loading in the steps of 20 kN; moreover, each loading step is executed in 5000 cycles (Fig. 2.14).

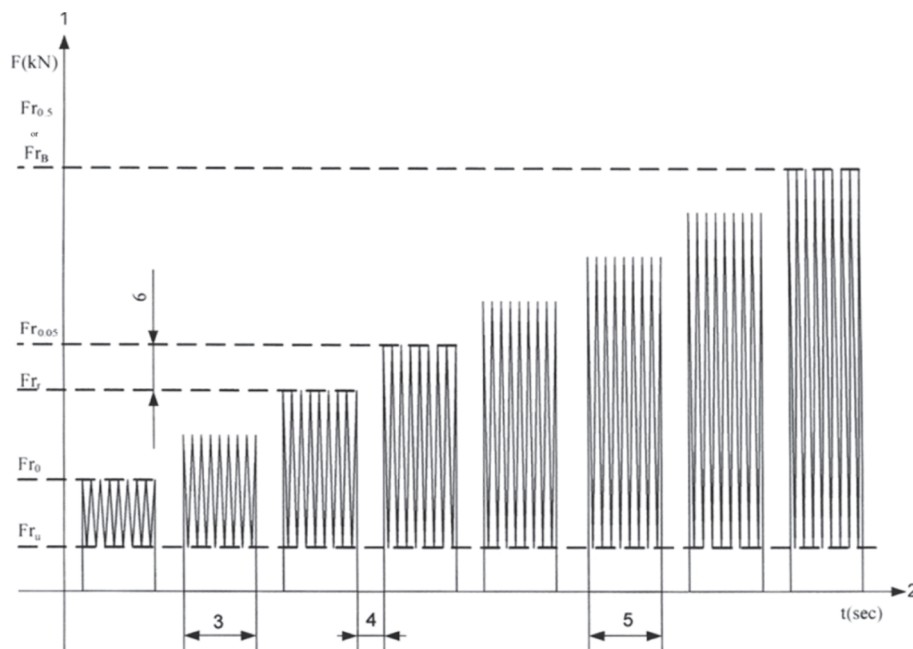


Fig. 2.14. Graph of the changes in the amplitude in the loading dynamic tests.

Afterwards, the step load is reduced to zero and the visual inspection of railway sleepers is made. The following parameters were determined step-by-step:

- 1) dynamic load, after removal of which a 0.05-mm wide crack remained on the lining of the sleeper under the rail;
- 2) dynamic load, which corresponds to the limit value of destruction, after the removal of which there persisted a 0.05-mm wide crack, which is also considered the destruction of the sleeper.

A crack width measurement was usually carried out at the end of the previous stages of fracture load using the Brinell microscope ($\times 24$ magnification; 0.05-mm scale interval). AE sensor was attached to the surface of the sleepers by means of a vibration-resistant adhesive such as “superglue”. For the comparative evaluation, three sensors at once were attached to the fourth sleeper according to Fig. 2.15(b). Sensors No. 1 and No. 3 were attached to the side surfaces of the sleepers, the sensor No. 2 was attached at the end of one of the reinforcement elements. As the analyzing equipment, the AF-3 device with a bandwidth of 20 KHz to 2 MHz was used (Fig. 2.15).

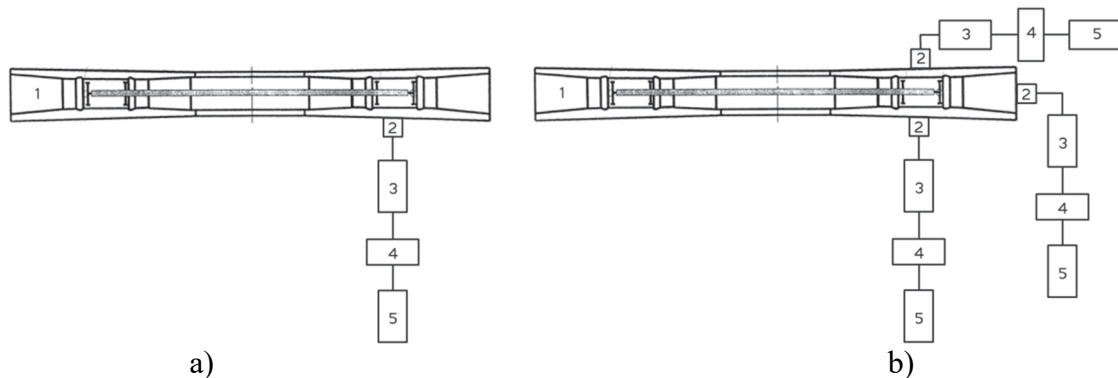


Fig. 2.35. Scheme of the location of sensors on the sleepers:

a) sensor installation on sleepers Nos 1–3;

b) sensor installation on sleeper No. 4.

Legend: 1 – sleeper; 2 – AE-sensor; 3 – preamplifier; 4 – AE unit; 5 – frequency unit.

As the controlling parameter, the cumulative AE count was chosen. The count was registered with the Ch-3-36 frequency counter.

CHAPTER 3: EXPERIMENTAL STUDIES OF THE MECHANISMS OF DAMAGE TO LAND TRANSPORT FACILITIES AND THE EVALUATION OF THE TECHNICAL STATE BY THE METHOD OF ACOUSTIC EMISSION

There are two key physical phenomena that may be used as evidence of the state of the material of the object tested. First is the AE event birth in the material under loading. The second is AE signal propagation features (refraction, reflection, decay, spectral changes, etc.). The absence of registered AE at the sensor may be the consequence of three major reasons:

- 1) lack of the sensitivity of hardware;
- 2) no presence of AE signals;
- 3) no AE pulse propagation between AE source and AE sensor.

The first reason may be revealed using calibration procedures. The absence of emission may mean, for instance, that the point of Kaiser [15] has not yet been reached in the material. The third case may be the evidence of damages in the material or in the material junctions (such as hollows, corruptions, etc).

If the emission is normally recorded during AE test, then different criteria are used to assess the stage of destruction and the state of material. Some of the criteria were based on AE event flow dynamic analysis (count, intensity). Other criteria may include the spectral analysis of signals.

In this chapter, the results of the AE assessment of land transportation objects are presented.

3.1 Application of AE in the assessment of Kegums HPP bridge

1. The defects such as cracks in the compounds bearing beams and bridge rivets internal fracture were not detected.
2. The greatest corrosive damage of all riveted joints of cover pads with beams was exposed to the 6th pad and especially to the 7th pad (see Fig. 2.2).
3. In the riveted joints of the lower pad and the beams, the joints Nos 1L, 1K, 2K, 4K, 5L, 6L, 6K and 7L had the most corrosive damage.
4. No significant influence of the degree of corrosion damage was observed on the technical condition of the bridge.

The carried out tests have confirmed the possibility of using AE technique in the assessment of the technical condition of hazardous buildings related to road infrastructure. The applied method of analyzing the amounts of AE signals with different joints is comparative. As was mentioned in the 1st chapter, AE is a passive method. It allows the registration only of those ultrasonic pulses that are produced in the material during the development of defects. However, in practical tests, the first part of the ultrasonic sensors was used as emitters. This is not a contradiction, because during the load test of the bridge it was necessary to understand how to interpret the absence of a signal on the sensor – either as the absence of AE or as the failure of emission signal to pass to the sensor due to corrosion.

The proposed and applied method is integral in the framework of the evaluation of the structure. This means that with the help of the same tool, both the degree of the development of visually detectable surface defects and the subsequent evaluation of the condition of the entire structure are checked. Moreover, the second stage of the evaluation is based on the results of the first one. In the second stage, if the acoustic emission pattern of the first beam with the same loading differs from the second one, a defect is present in the beam with a higher emission intensity. It is for this purpose that the first stage is necessary – to exclude the influence of external corrosion and other defects on the AE pattern.

Thus, the proposed method is a method of simultaneously obtaining both a pattern of AE data verification and the data itself. The numerical value of the degree of correspondence, expressed through an appropriate mathematical tool, i.e., the RMS pattern and data vector, is the criterion for assessing the state of the structure. Any other NDT method would not allow such an assessment of the object “entirely”.

3.2 Assessment of the 2M62 locomotive bogie frames and bolsters

Test results and analysis. Fig. 3.1 shows the variation of AE parameters depending on the time under bolster cyclic loading to failure under the program referred to in Chapter 2. Fig. 3.2 shows the same graphs but the initial time of loading at an enlarged scale with respect to time. It is evident that a fast growth in the cumulative AE appeared which is the point of $\alpha_{\text{criterion}}$. The intensity of AE increased sharply at the time of the relevant operating time of 48 000 cycles. This AE behavior is characterized by the fact that at the time of abrupt changes of AE parameters, a fatigue crack appeared.

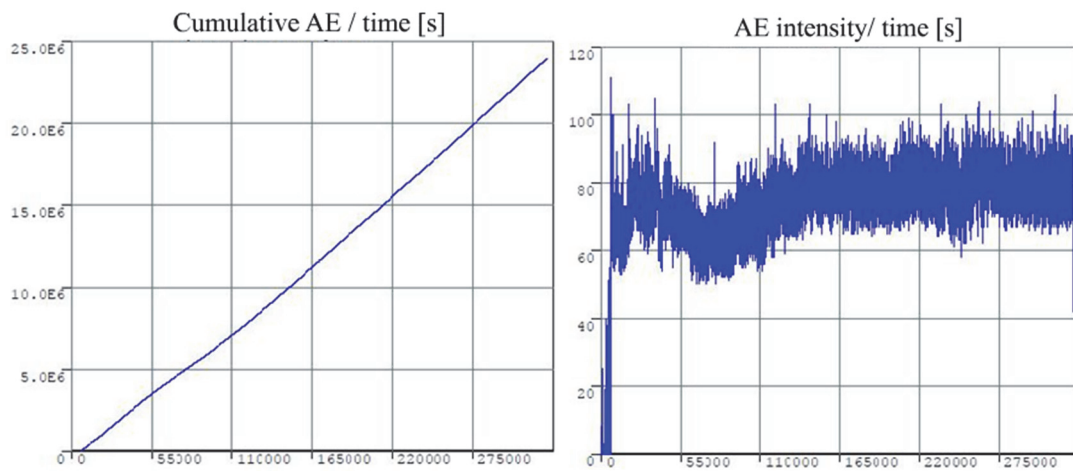


Fig. 3.1. Graph of cumulative AE (left) and intensity (right) under bolster cyclic loading to failure.

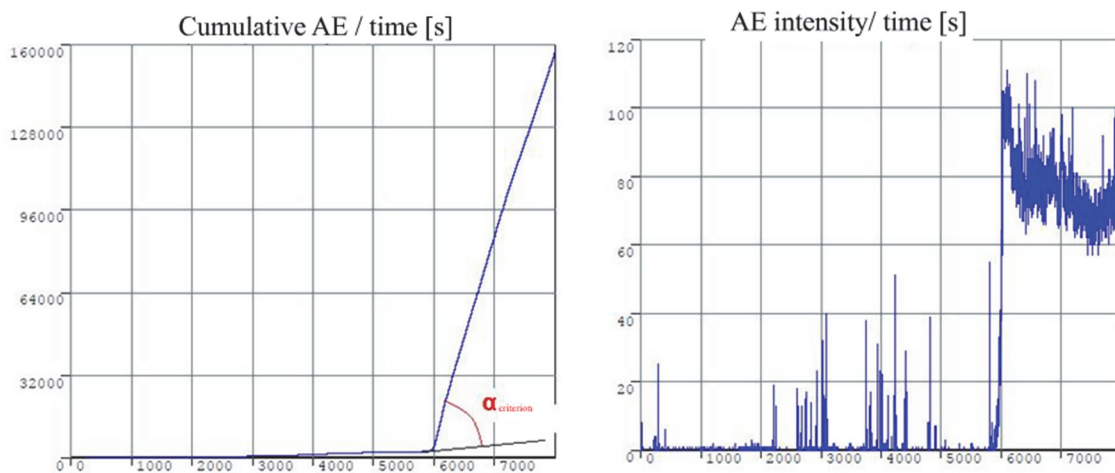


Fig. 3.2. Graphs of the change in cumulative AE (left) and intensity (right) at the stage of the occurrence of a fatigue crack in the bolster under cyclic loading.

Test result summary., The problem of determining the state of cast parts bogie was successfully solved by AE method. Thus, AE method allowed determining the occurrence of fatigue cracks much earlier than the visually (optically). Tests showed the descriptiveness of the AE dynamic criterion in the problem of determining the stage of the damage during the fatigue tests of bogie frames and bolsters.

3.3 Features of the behavior of AE signals at the dynamic bench tests of prestressed concrete sleepers

Test results and analysis. The destruction of the sleepers Nos 1–3 happened under the dynamic load of 250 ± 200 kN on the 18th stage. The destruction of the sleeper No. 4 happened on the 14th stage with a load of 200 ± 150 kN. Visual inspection during routine checks discovered the occurrence of cracks with the coast opening of the magnitude of 0.05 mm in the sleeper No. 1 after the 8th stage of dynamic loading. On the sleepers Nos 2–3, the destruction was discovered after the 15th stage. On the sleeper No. 4, such wide end opening to the fracture was not detected till the end of destruction. Fig. 3.10 shows an example of the photographs of sleeper No. 1 shortly after the 17th stage of loading.

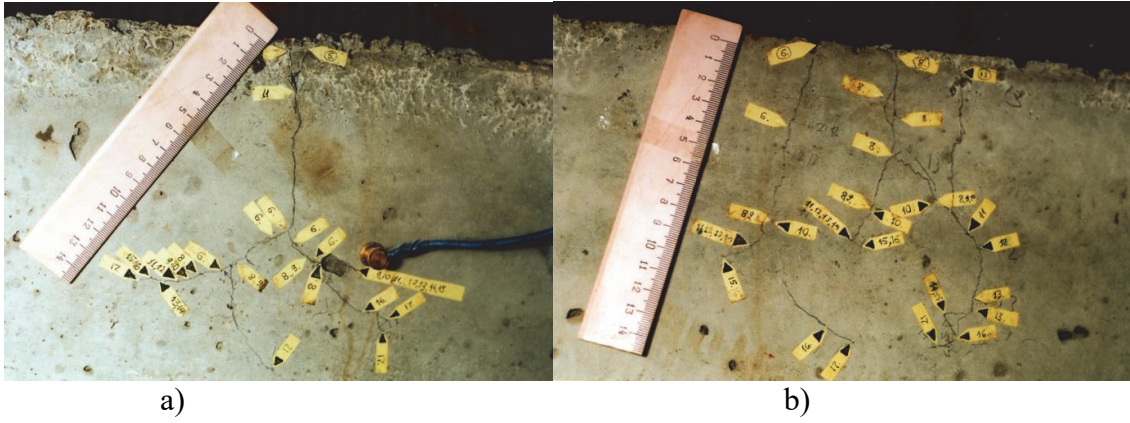


Fig. 3.3. View of the cracks on the side surfaces of the sleeper No. 1 after the 17th stage:
a) left side; b) right side.

The analysis of the dependence of cumulative counting and the intensity of the dynamic loading (see Figs 3.4–3.7) demonstrate a clear relationship between the AE signals and the durability of the sleepers tested.

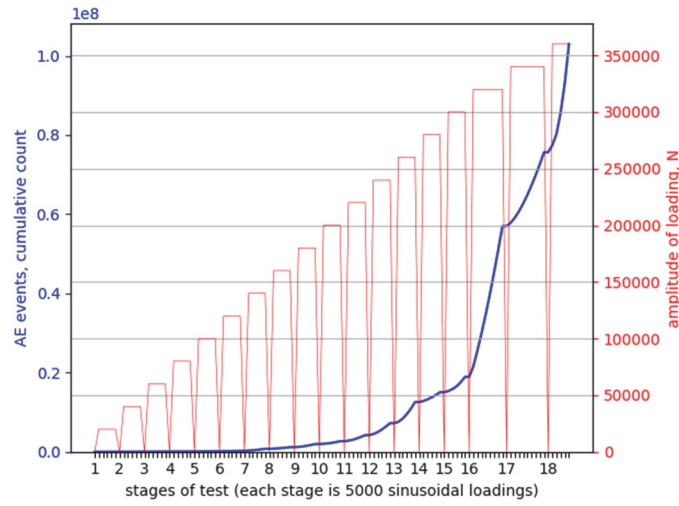


Fig. 3.4. Cumulative AE count and AE intensity on sleeper No. 1.

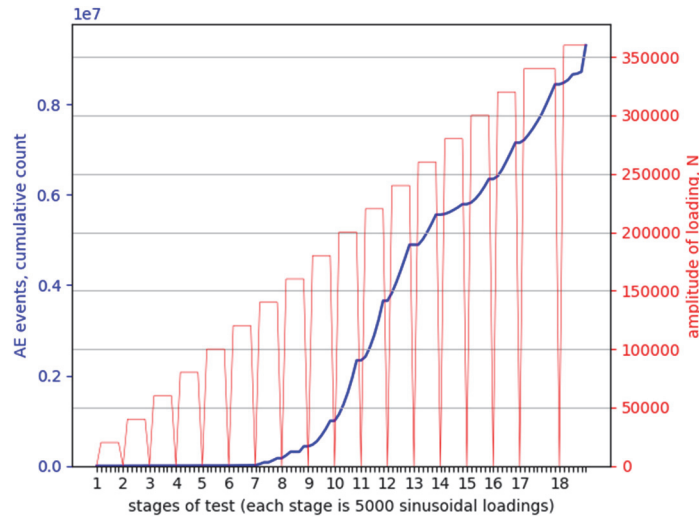


Fig. 3.5. Cumulative AE count and AE intensity on sleeper No. 2.

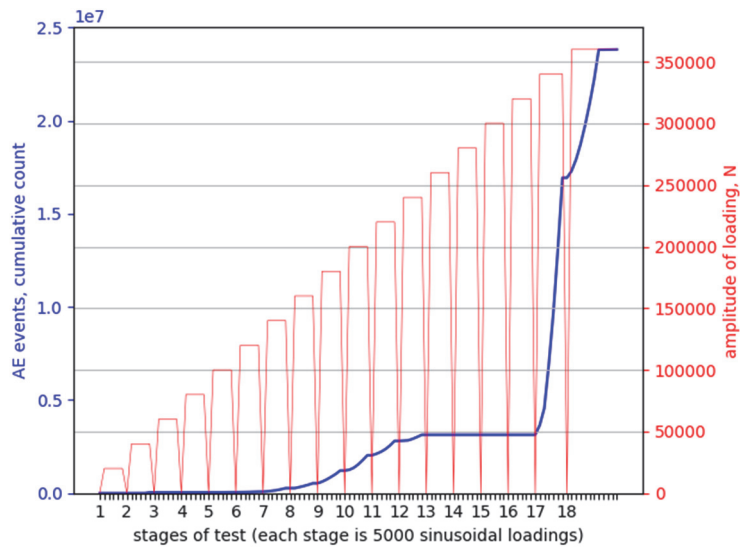


Fig. 3.6. Cumulative AE count and AE intensity on sleeper No. 3.

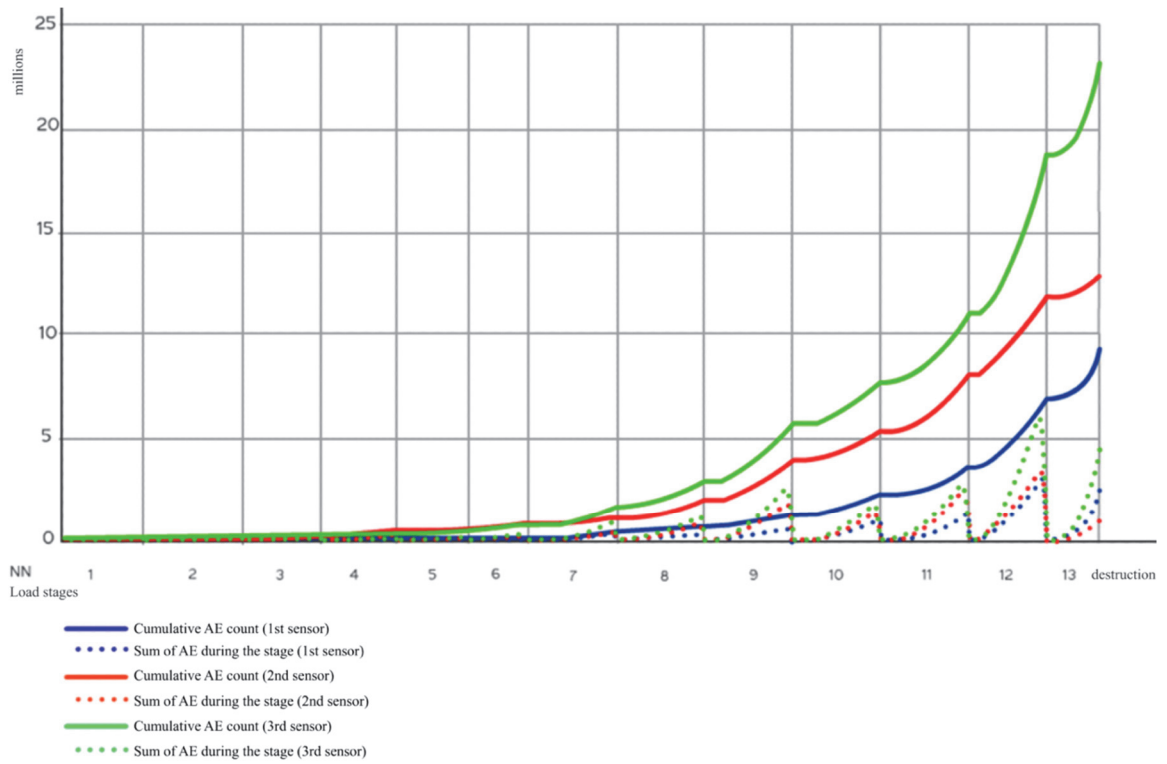


Fig. 3.7. Cumulative AE count and AE intensity on sleeper No. 4 (three sensors).

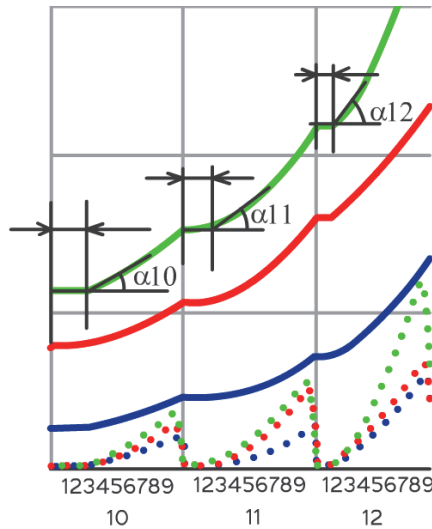


Fig. 3.8. Fragment of the cumulative AE change on the load stages Nos 10–12.

The identical behavior of cumulative AE during dynamic loading from stage to stage is evident (see Figs 3.4–3.7). Thus, each stage of dynamic loading can be divided into two sections of the behavior of the total AE (Fig. 3.8): the stage of slow (weak) growth and fast growth (rapid) increase with the form of angle α .

This behavior can be explained as follows. In [6] it is shown that the formation of the angles α in metallic materials is associated with the moment of the formation of microcracks, i. e., with the destruction process in microvolumes. In this case, during the control of the width of the crack opening, the compressive force manages to partially restore structural integrity to the atomic level. Therefore, the beginning of each stage is accompanied by a low cumulative AE, because there no new cracks have been formed yet.

Test results and analysis

The experiment data make it possible to use the following three classification features (Fig. 3.9). The first feature is the number of loading cycles from 0 to M_1 , which stands for the plateau at the graph of cumulative AE. The second classification feature is the amount of loading cycles between M_1 point and α -criterion onset point. The third is the α slope.

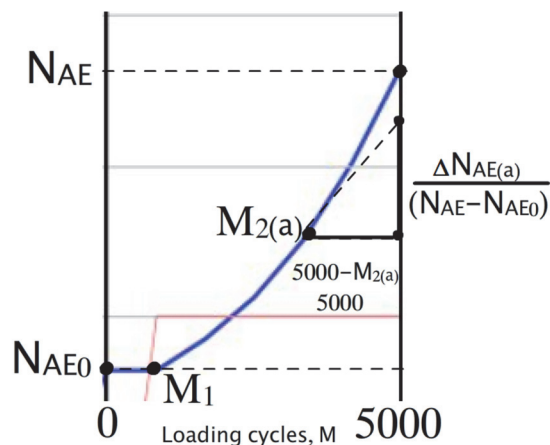


Fig. 3.9. Diagnostic test pattern classification features.

Eighteen supervised classes corresponded to the same amount of healthy sleepers loading programme stages. The training set was based on the data of 11 samples. For each of the 18 stages of loading, an observation vector v made with an intention to do assignment v to one of the 18 classes was recorded.

After gathering the classification patterns, all recordings on 11 healthy sleepers were verified for compliance to the rest 10 patterns. In order to do so, the decision rule was used: the probabilities to assign v to class j . If the probability φ_j for the taken recording is greater than all classes $\varphi_1 \dots \varphi_{18}$, then v is assigned to class φ_j :

$$P(\varphi_i | v) > P(\varphi_j | v) \quad j=1, \dots, C; \quad i \neq j, \quad (3.1)$$

where C – number of classes;
 j – ordinal number of the class.

Table 3.1. Prestressed concrete sleeper's health classifiers (average) for 11 sleepers

Class	Classification feature			Structural health assessment of sleepers
	Feature 1: The length of plateau, loading cycles, N	Feature 2: Number of cycles between plateau end and α feature onset, N	Feature 3: intensity/cycles in relative coordinates, $\text{tg}(\alpha)$	
1	4583	251	1.4	94 %
2	4250	247	1.4	89 %
3	4167	241	1.4	83 %
4	1667	233	1.8	78 %
5	1500	223	2.2	72 %
6	1167	211	2.6	67 %
7	1083	190	3.0	61 %
8	1000	174	3.3	56 %
9	917	156	3.8	50 %
10	833	136	4.0	44 %
11	750	103	4.0	39 %
12	583	79	5.0	33 %
13	417	53	5.4	28 %
14	250	25	5.8	22 %
15	167	12	5.9	17 %
16	83	4	6.6	11 %
17	75	4	7.0	6 %
18	42	3	7.4	Near destruction

After this, the Baye's rule for minimum errors was used [23, p. 13]:

$$P(k) = \sum_{i=1}^{18} P(k|v_i)P(v_i) . \quad (3.2)$$

The error for each of 18 pairs of “vector of features/training set vector” was calculated as follows:

$$k_j = \frac{1}{n} \sum_{i=1}^n \frac{1}{\left(\frac{|\varphi_{i,j} - v_i|}{\max(\varphi_{i,j} - v_i)} + 1 \right)}, \quad (3.3)$$

where n – number of classification features (length of vector v);
 i – ordinal number of the classification feature;
 j – ordinal number of the class;
 v_i – i -th feature of vector v for the assessed object;
 $\varphi_{i,j}$ – i -th feature of vector φ for the corresponding class.

Method verification

To verify the described approach, the following steps were made:

- 1) all recorded training data for 10 healthy sleepers and for 1 defective sleeper for every of 18 loading steps was used for verification. Here and below: a sample is one loading stage test for one sleeper; The total amount is $11 \times 18 = 198$ samples;
- 2) in the process of verification of the sleeper N, the data of N-th sleeper was excluded from the training set. Then, each of 18 vectors of N-th sleeper was compared with the rest of the training samples using formula (3.3);
- 3) training sample with the least error-value was determined as classified;
- 4) the same steps 2 and 3 were done for other sleepers. Classification data is the following:

Number of positive samples [17] (P): 161

Number of negative samples (N): 20

Number of true positive (TP): **180**

Number of true negative (TN): **18**

Number of false positive (FP): 2

Number of false negative (FN): 19

False positive rate (type I error): $FP/(FP+TN) = 10\%$

False negative rate (type II error): $FN/(TP+FN) = 9\%$

Classification accuracy: $(TP+TN)/(TP+FP+FN+TN) = 90.4\%$.

Conclusion. In order to quantify the breaking load in the prestressed concrete sleepers, tests with loading have been conducted. During the tests using the method of AE, initial (primary) crack, crack opening, and destruction were identified. This indicates that the AE method allows determining the beginning of the formation and then the development of a crack at an earlier stage than it is possible to do by other methods of instrumental and visual inspection.

During visual inspection, at intervals of no more than five minutes between the steps of dynamic loading, there was “healing” of the shores of opened crack. This effect is clearly seen in the diagram of AE signals during the transition to the next loading step. Fracture “healing” time decreased with each successive step. The results obtained allow further determining the quality of adhesion of the concrete with reinforcement, thus assessing the quality of the manufacture of any structures of prestressed concrete.

CHAPTER 4: INVESTIGATION OF THE DAMAGES OF MODERN COMPOSITE MATERIALS AND DEVELOPMENT OF ASSESSMENT CRITERIA USING THE SPECTRAL PROPERTIES OF AE SIGNALS

4.1 Description of the subject area

The term “composite” in terms of composite materials means two or more materials combined at a macroscopic level in the form of the third material having new and useful properties. The use of composites in transport is relevant in connection with the ever-increasing demands for productivity and security. For example, there is a partial replacement of structural elements on cars with traditional composite counterparts. Among the elements that in modern rail cars are made of composites, the following can be mentioned: shutters and latch windows, window sills, guide rails for the moving parts of windows, window frames, modular toilets, main doors. Boxes and battery compartments are already in large numbers are made of fiber-reinforced plastic (FRP – fiber-reinforced plastic) [4]. There are examples of composites based on epoxy resin, and FRP-composites in the manufacture of sleepers. In India, which has the fourth largest railway network in the world [16], there was successfully tested the practice of the use of FRP-composite sleepers on the railway girder bridges to reduce the use of wood. Australia started the use of the sleepers made of epoxy resin on the matrix of the polymer concrete [8].

Among the circumstances that prevent the spread of the use of composites in the construction of road infrastructure, the researchers mention the lack of simple and reliable methods of inspection

of composite objects and procedures for their repair [18]. This indicates the need for the development of real-time nondestructive testing and monitoring techniques applied to composite objects. AE method can be a tool for the detection of defects in composite elements in the earliest stages.

4.2 Material characteristics

The following materials were used in the study:

- 1) epoxy filled composition (epoxy resin Araldite® LY 1564/Aradur® 3486) with different filler content;
- 2) filling: polyethersulphone brand Ultrason® E 2020 P SR micro (PES).

The investigated epoxy resin composition has a content of the PES weight of 0.0 %, 5.0 %, 7.5 %, 10.0 %, and 12.5 %, and it is obtained by mixing in a conventional mixer at room temperature for 30 minutes and cured in accordance with the rules for four hours at a temperature of 100 °C.

4.3 Research objectives

1. To determine the effect of filler concentration on the fracture toughness and simultaneously determine the possible mechanisms of the microfracture of epoxy resins with different content in the matrix of particulate filler.
2. Using the analysis of AE signals, to determine the characteristic pattern of the order of the sequence of microfracture processes.
3. To determine the behavior of the α -AE criterion in the composite material, for example, epoxy composite PES-filler.
4. To determine the spectral characteristics of AE signals in destructing composites.

4.4 Test methods

To determine AE characteristics of the composite structures, it is important to determine them for the source material. In tests, the epoxy composite PES-filled samples used for stretching to break (see Fig. 4.1).

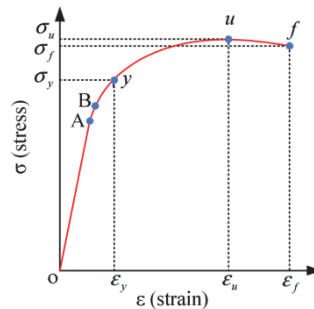


Fig. 4.1. Strain/stress curve:

- σ_u – tensile strength;
- σ_f – fracture stress;
- σ_y – yield strength;
- ϵ_u – uniform strain;
- ϵ_f – strain to fracture;
- ϵ_y – yield strain.

Samples. In tests, 30 composite samples of the sizes 2 mm × 10 mm × 150 mm (Fig. 4.3) with varying concentrations of PES (0.0 %, 5.0 %, 7.5 %, 10 %, and 12.5 %) were used.

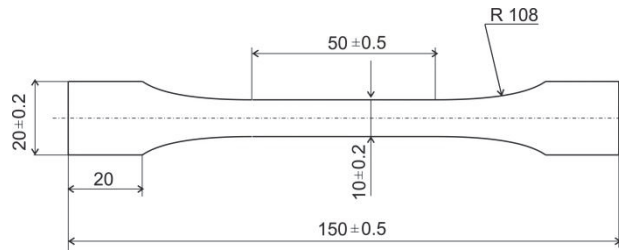


Fig. 4.2. The test sample (dimensions in mm).

Test procedure: Tensile tests were performed on the test machine Zwick/Roell 2,5 using the maximum load of 2.5 KN. The tensile test was chosen due to the uniformity of distribution across the sample stress. The testing machine crosshead speed was 2 mm/min. Before the test, the AE sensor model R6-ALPHA of the company “Mistras Group” was joined to the sample. The unit AE model MICRO-II of the “Mistras Group” was used to measure the acoustic signals. Before testing, the samples were conditioned at the temperature of $+22 \pm 2$ °C and the relative humidity of 50 %. In the tests, the values of the applied load, the deformation of the specimen, and the AE signals were recorded. According to the test results of the samples, the strength tensile strain limit and the modulus of elasticity were calculated

In all cases, the duration of the experiment was different. In this case, the elongation and the load at sample rupture time were also varied. This created a difficulty in comparing the dynamics of the emergence of AE pulses between both groups of samples with different concentrations of PES, as well as between the samples of the same group. To solve this problem, it was proposed to shift the coordinate system from the absolute time into the relative coordinate system (normalization) in the time domain where 0.0 is the beginning of the experiment, and 1.0 is the time of sample fracture (the mathematical model is discussed in Chapter 5). To implement this, a software was developed in the research. An example of the combined normalized data from AE MicroII computer and data from the testing machine is shown in Fig. 4.3.

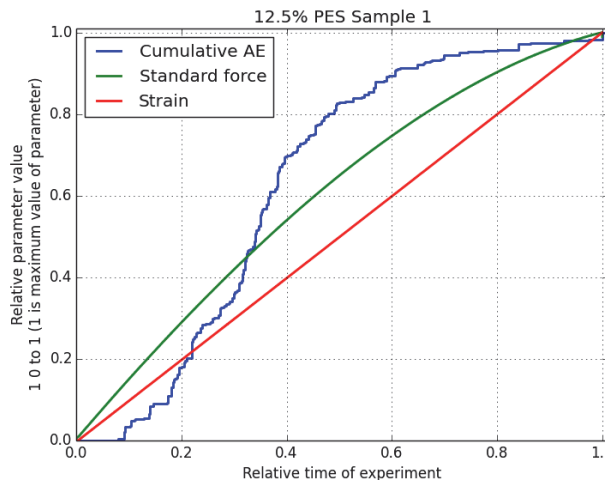


Fig. 4.3. The normalized representation of the experimental data on the sample No. 1 at the PES concentration of 12.5 %.

Then, for each group of the same PES concentration samples, the average values of AE and tensile load in the time domain were calculated. In each of the sample groups, α_1 and α_2 points were defined. The results obtained for the samples of groups with PES concentrations of 0.0%, 5.0%, 10.0%, and 12.5% are shown in Fig. 4.4.

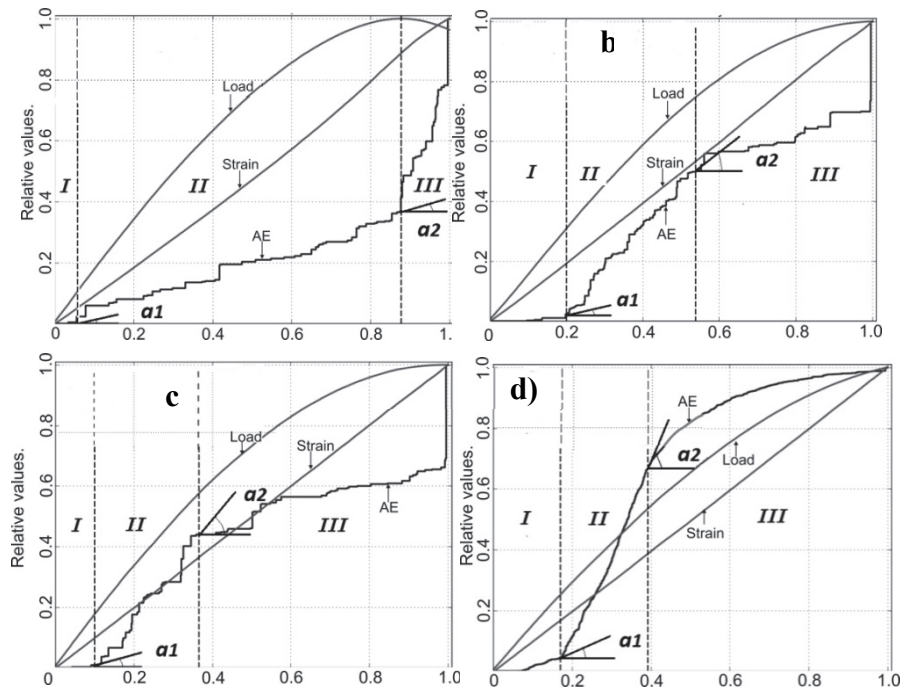


Fig. 4.4. The average results of the experiments for all sample groups:
a) pure epoxy resin (0.0 % PES); b) PES – 5.0 %; c) PES – 10.0 %; d) PES – 12.5 %.

The analysis of the results allows drawing a preliminary conclusion that the different concentration of the filler of the PES leads to different scenarios of the destruction of the material. Thus, at least three different phases of the accumulation of microfracture were revealed: 1st – initial (0.0–0.2 time to failure, for example, see Fig. 4.4.b), when there is no significant accumulation of damage in the material; 2nd – the stage of moderate formation of defects, when the rate of AE accumulation increases. There is a break of the weak adhesive bonds between the filler and the matrix on the stage:

- 0.20–0.40 as in Fig. 4.4.(d) (PES – 12.5 %),
- 0.20–0.55 as in Fig. 4.4.(b) (PES – 5.0 %),
- 0.10–0.35 as in Fig. 4.4.(c) (PES – 10.0 %),
- not observed in the group of the samples without PES.

In addition to the analysis of AE as a stream of discrete events, an analysis of the spectral characteristics of AE pulses emitted by a degradable material was also carried out. During the experiment, the waveforms of the AE pulses were recorded and then analyzed with the help of the software developed within this Thesis.

There were investigated:

- 1) spectral characteristics of individual events (Fig. 4.5);
- 2) distribution of the energy spectra of frequencies by the time of the experiment (Fig. 4.6);
- 3) distribution of the maximum energy of the frequency spectrum in the time domain (Fig. 4.7).

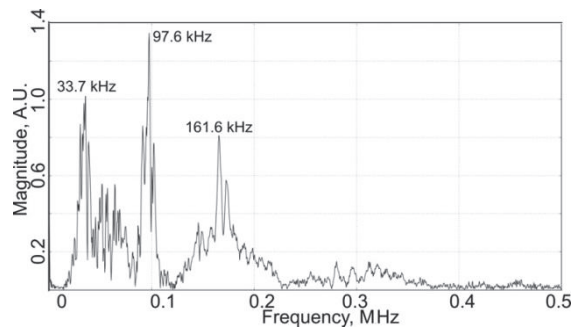


Fig. 4.5. Spectral density of a single AE event in a crumbling composite.

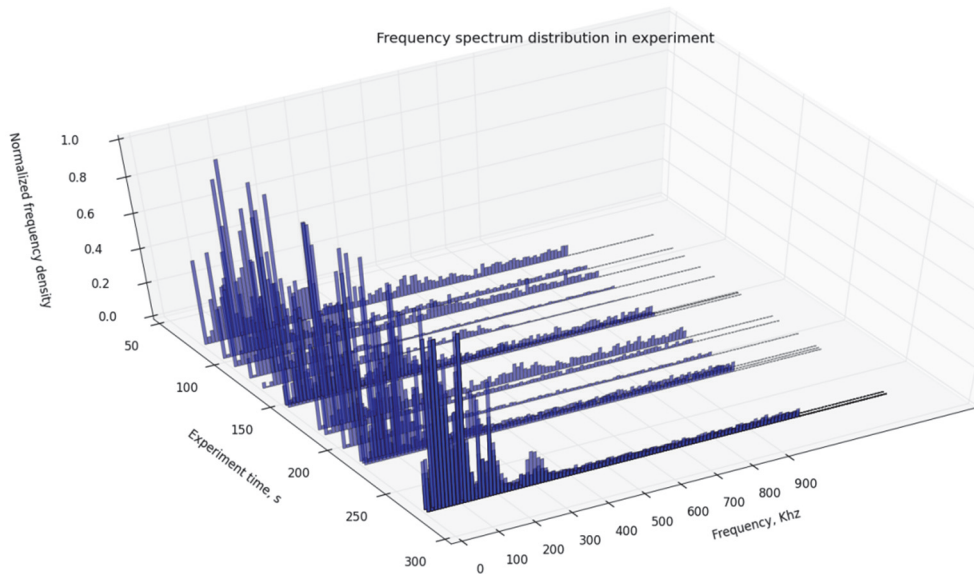


Fig. 4.6. Frequency distribution of the energy spectra of all events during a single experiment.

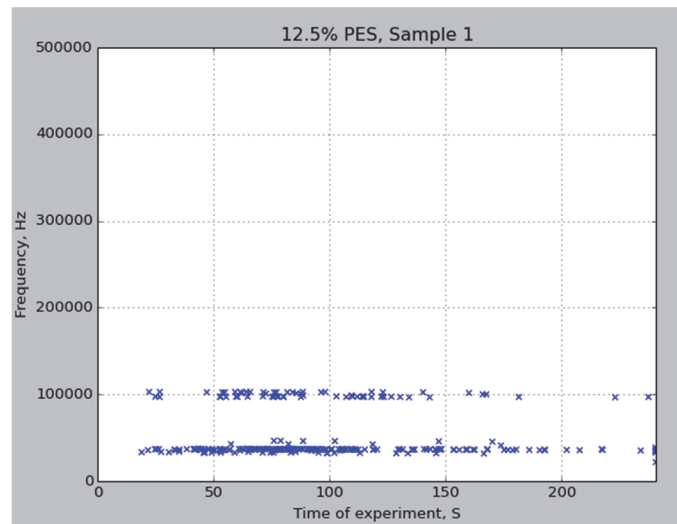


Fig. 4.7. Maximum energy distribution in the spectrum of the frequencies of all events in the coordinates of time.

4.5 Test results

As a result of AE method application, it is possible to make several conclusions.

The analysis of the cumulative AE count indicates the existence of three different stages of the accumulation of damage in the composite. These steps cannot be identified by using only the strain diagrams but they are distinguishable on the AE diagrams. The time of the onset of these phases is determined by the moment of manifestation of the criteria α_1 and α_2 .

In PES-modified composites, the process of damage accumulation becomes evident from 10–20 % of the ultimate strength of the load. At the same time, in pure epoxy matrix, the process becomes evident only with 85 % load.

Characteristics of the spectrum frequency of AE signals are changed in the process of passing the stages of the destruction of the material and can be used as an additional parameter assessment of the state of disintegration. It was found that the average frequency of maximum spectral power at the end of each experiment is lower than at the beginning.

4.6 Summary of Chapter 4

It was found that the manifestation of α_1 - and α_2 -criterion of defects in the composite material is linked to the general picture of the behavior of this criterion in the objects studied in Chapters 2 and 3 (materials: concrete, steel) as well as in the earlier studies. Thus, there is a reason to assume that this criterion can be used as a universal indicator in determining the state of the structures and units made of all major materials used in transport: concrete, metal, polymer composites.

The software developed by the Thesis' author has helped to identify the relationship of the spectral characteristics of the AE signal in the composite with the appearance of a particular stage of α -test. This question is discussed in detail in Chapter 5.

CHAPTER 5: MATHEMATICAL ANALYSIS OF THE SPECTRAL AND DYNAMIC CHARACTERISTICS OF AE SIGNALS AND DEVELOPMENT OF A MATHEMATICAL METHOD FOR IDENTIFYING THE STAGES OF MATERIAL DESTRUCTION

5.1 Problem description

High-quality collection of information on the state of buildings and structures by AE is a key condition for the possibility of predicting the durability of an object. During the test sites and materials listed in Chapters 2–4 and in other experimental studies involving the author, several practical problems of data collection and analysis were ascertained.

1. During AE testing of large objects such as bridges, wagons, and tanks, a need arose for the simultaneous use of a large number of sensors. The presence in the laboratory of AE devices with a large number of channels does not guarantee that the experiment of required scale can be delivered using a single AE computer. At the same time, it is practically difficult to implement simultaneous AE data reading with using multiple AE devices.
2. It is shown in the work that the technique of using alpha-test as an indicator of the onset of a new stage in the destruction may help in assessing the status of objects, but is rather non-trivial and requires analytical work on data interpretation. However, there is no ready software solution to more clearly define the time of α -criterion in experiment.
3. The fact that alpha-criterion identification itself does not make it possible to determine which stage of the destruction has passed until the next stage starts. There must be a connection of this criterion with some additional parameter, which would help identify the specific stage of destruction, indicated by the amount of emissions' growth rate.

In this Chapter, the practical steps for a possible solution of these problems are shown

5.2 The problem of the compatibility of AE systems

The developed program is a script written in the language *Python 2.7*. The Python ecosystem is one of most exploited in scientific programming, along with the family of *Matlab*, *MathCad*, *StatGraphic*, *Catman*, etc. The script can be run on a computer running any operating systems *Windows*, *MacOs*, *Linux*, *Unix*, *Android*, *iOs*, and others. The software was developed and then tested and used in the research described in Chapter 4. All the following results in this Chapter correspond to the experiments with PES-composites.

5.3 Data normalization function

Each experiment in each composite sample group had a unique time of the occurrence of the rupture of the sample, as well as a unique score of AE at break. Conducting a comparative analysis of such experiments without reduction to a single scale is difficult. In order to solve this problem, a normalization method was proposed by which all time and AE count data were re-calculated from the absolute values to the relative ones, at the time axis, and at the cumulative AE axis where the zero is the beginning of the experiment, and 1 - the experiment end (sample break).

This was done as follows: an array of the data readout time of the registration of AE signals is the vector t_k :

$$t_x = \langle t_{x,0}, t_{x,1}, \dots, t_{x,n-2}, t_{x,n-1} \rangle, \quad (5.1.)$$

where x – serial number of the experiment in group;
 n – number of registered AE count changes.

Each value of t_x vector corresponds to the value of c_x vector (cumulative count), which determines the cumulative AE count at the moment of time:

$$c_x = \langle c_{x,0}, c_{x,1}, \dots, c_{x,n-2}, c_{x,n-1} \rangle, \quad (5.2.)$$

where n – number of registered AE count changes;
 x – serial number of the experiment in group;
 $c_{x,i}$ – cumulative AE count value at the time moment $t_{x,i}$.

Normalized values of the time determined by the vector t_x^{norm} :

$$t_x^{norm} = \frac{t_x}{\max t_x}, \quad (5.3.)$$

where x – serial number of the experiment in group;
 t_x – vector of time values before normalization.

The normalized cumulative AE count values are determined by the vector c_x^{norm} :

$$c_x^{norm} = c_x / \max c_x, \quad (5.4.)$$

where x – serial number of the experiment in group;
 c_x – cumulative AE count value before normalization.

Thus, after performing the normalization, the time data and counting all experiments AE converted into relative coordinates.

5.4 Determination of the dynamic α_1 and α_2 criteria using the “smoothing” function

The fracture criterion (α -test) is determined by the sum of the positive increments of AE curve, which at some point has a bend. The increment represents the change in the dynamics of summed AE signals. Due to the lack of expressed linear areas on the graph of total AE, it is difficult to use the alpha test for the detection of the moment of occurrence of a fatigue crack. In this connection, a convenient indicator of the occurrence of a fatigue crack is the second derivative of the total registered AE.

In the calculation of the second derivative, depending on the operating time not graphically but by direct differentiation in certain time intervals, the high sensitivity of this test to change the dynamics of total AE provides a large number of the areas of the sign change at the stage of the accumulation of fatigue damage.

To solve this problem, it was proposed to the inertia element in the graph of total AE smoothing method. The smoothed normalized vector of the total value of AE c'_x is generally calculated as follows:

$$c'_{x,j} = \frac{\sum_{i=j}^{k+j} c_{x,i}^{norm}}{k} \\ c'_x = \langle c'_{x,j} \rangle; j = \langle 0, 1, \dots, n - k - 1 \rangle, \quad (5.5.)$$

where k – number of the elements of the smoothing window;
 n – number of registered AE count changes;
 x – serial number of the experiment;
 $c_{x,i}^{norm}$ – value of cumulative AE in the x -th experiment at the time moment $t_{x,i}$.

After smoothing the input vector account acoustic emission resulting vector c'_x , length of n elements is fed to the input of the digital differentiation function, which is calculated using the length of the vector $n-2$, which is a derivative of the second order along the time axis:

$$\alpha_x = \frac{\partial^2 c_x'}{\partial t^2}, \quad (5.6.)$$

where a_x – the resulting vector.

The differentiation is carried out by the function *diff* from *numpy* library. The resulting vector a_x is also fed to the input of the smoothing function described above, and based on the result of the graphical representation of the second derivative, the total AE, elongation and stress in the system of relative coordinates are built (Fig. 5.1).

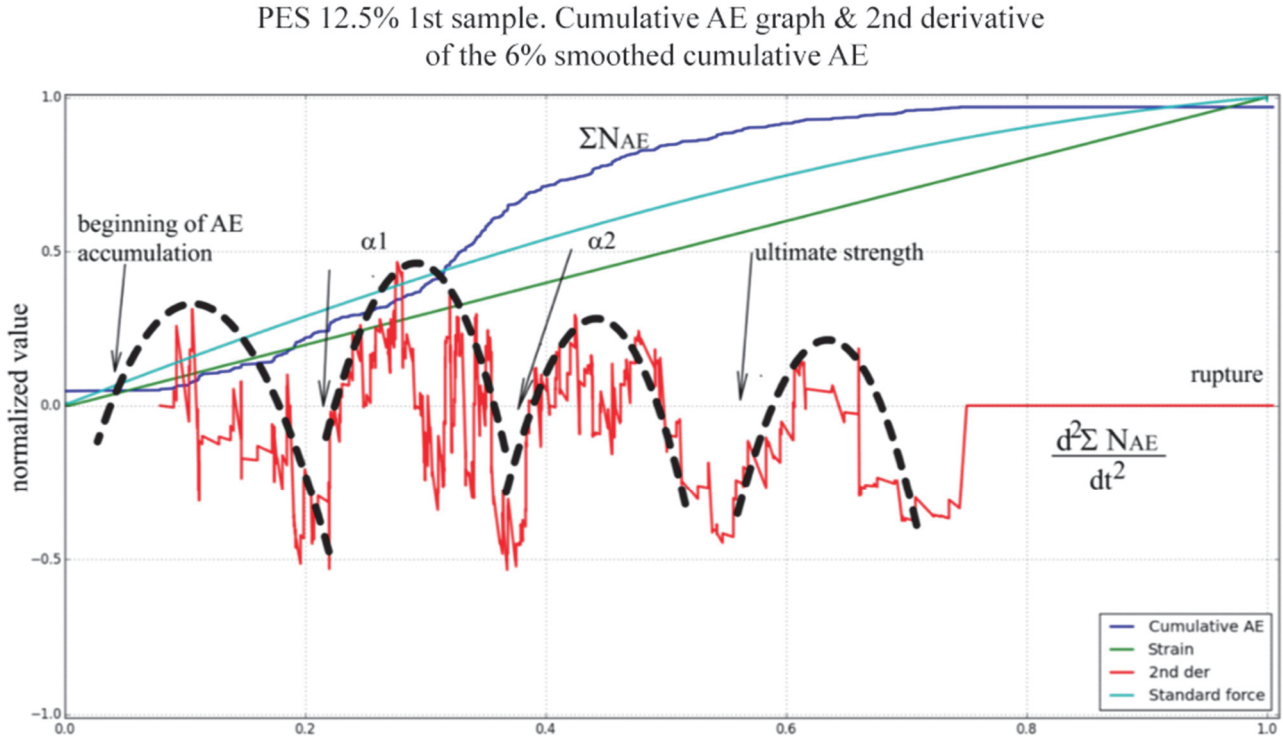


Fig. 5.1. Total AE and the second derivative of the smoothed total AE array obtained by direct differentiation.

Figure 5.3 shows the result of an experiment for the composite sample containing 12.5 % PES. The dotted line indicates four expressed zones of the rise and fall of the second derivative of the total AE, wherein the smoothing function window to the 6 % of the length of the experiment is applied as to the initial AE, i.e., to its second derivative. Start rise of the first zone corresponds to the start of the accumulation of AE. Subsequent to this recession and the beginning of the second lifting, zones correspond to α_1 . The joint between the second and third zones indicates α_2 , and, finally, the last rise coincides with the achievement of the ultimate strength. Similarly, the data have been processed for all the other experiments' composites containing 0.0 %, 5.0 %, 7.5 %, 10.0 %, and 12.5% PES. The data obtained showed satisfactory agreement between the dynamics of the 2nd derivative of the total time of the AE occurrence of the phases of all these stages. Thus, the problem of the complexity of the interpretation of the amount of the rate of the increase in AE has been solved, and it made the α -criteria visualization more informative and an easy-to-read indicator of the developmental stages of destruction.

5.5 Development of the program of AE frequency analysis

Industrial software allows visualization of the data of only those experiments that are recorded directly to these programs. For group analysis of the AE-data that was recorded using different AE-hardware, the new software for analyzing dynamics of AE-parameters was developed. It allows analyzing the spectral characteristics of the AE, and it is necessary to identify the patterns between the intensity and the frequency of AE signals.

Spectrum analysis is performed by discrete Fourier transforms. Fourier theory postulates that a certain signal can be reconstructed by summing sine waves of different amplitude, frequency, and phase. Thus, the input signal is in the time domain, and both of the output signals are in the frequency domain. Using a Fourier transform, the time domain signal is transformed to the frequency domain, which is equivalent to the amplitude spectrum and phase spectrum. On the basis of DFT output function builds a range of signal power density was built. (Fig. 5.2).

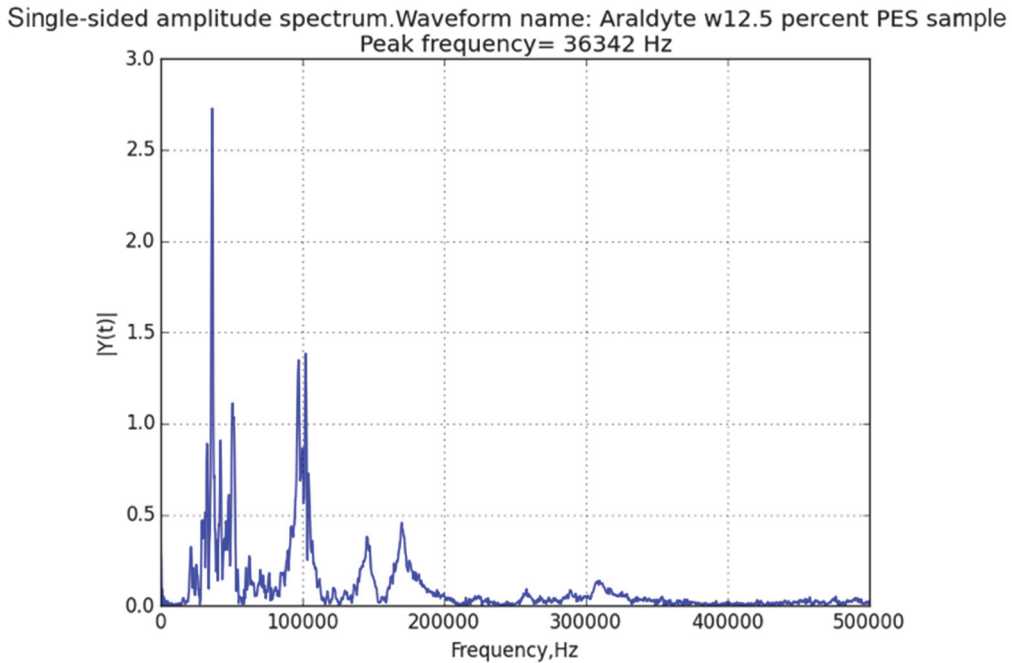


Fig. 5.2. DFT¹ spectral decomposition excluding the imaginary part with an indication of the “peak” of the frequency spectrum.

5.6 Determination of the maximum frequency power spectrum density

The result of the discrete Fourier transform is a vector of the values of the amplitudes of the frequencies defined in increments. This allows determining the maximum rate for each AE event in the experiment. A frequency maximum spectral power density distributed over time generates a picture of the experiment (Fig. 5.3).

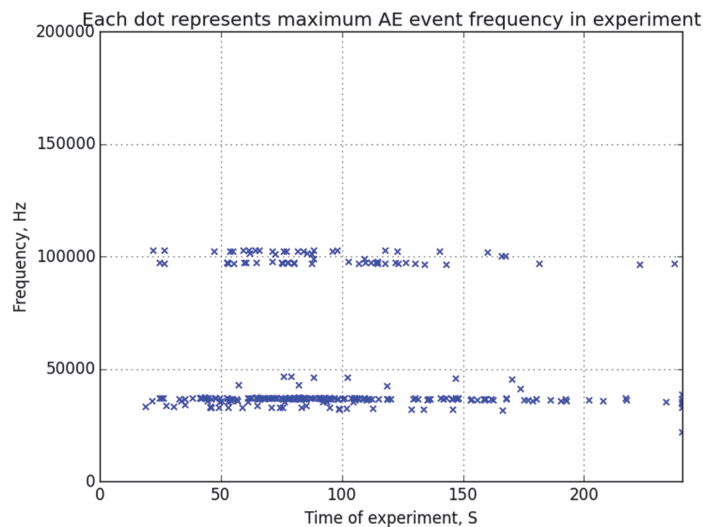


Fig. 5.3. Distribution of the maximum power spectral density.

¹ DFT – Discrete Fourier Transformation

Each AE event is indicated on the chart by one point. It is noticeable that the events are divided into two narrow zones, and there are no intermediate values between them. It is also possible to notice that at different stages of the destruction of the composite sample (the test method is described in Chapter 4), the maximum frequency of the picture is changing. This change has been used as a **new parameter** in the study of the dynamics of the amount of AE.

5.7 Determination of α -criterion connection with the spectral characteristics of AE signals during the destruction of epoxy composite

The developed software allows analyzing the dynamics of the AE parameters and their connectedness. The analysis of the frequency characteristics of AE disintegrating the PES composite revealed that in all cases when testing composite samples, the accumulation of AE was accompanied by the decrease in the frequency of the maximum spectral power density of the events from the beginning to the end of the experiment. In each experiment, two points were observed expressed by increasing the rate of the growth of the cumulative AE designated as α_1 and α_2 . The change in the peak frequency of AE was uneven.

In order to determine the behavior of the maximum frequency, it was proposed to use a polynomial approximation of a function (fit-function).

In general, the fit-function is written as follows:

$$f(x) = a_0 + a_1x^1 + \dots + a_jx^j = a_0 + \sum_{k=1}^j a_kx^k \quad (5.7.)$$

where $a_0 \dots a_j$ – coefficients;

j – order of polynomial.

To minimize the mean square error of approximation functions, the partial derivatives of the expressions for these coefficients were assigned to zero values:

$$\begin{cases} \frac{\partial \Pi}{\partial a_0} = -2 \sum_{i=1}^n [y_i - (a_0 + \sum_{k=1}^j a_k x^k)] = 0 \\ \frac{\partial \Pi}{\partial a_1} = -2 \sum_{i=1}^n [y_i - (a_0 + \sum_{k=1}^j a_k x^k)] x^1 = 0 \\ \vdots \\ \frac{\partial \Pi}{\partial a_j} = -2 \sum_{i=1}^n [y_i - (a_0 + \sum_{k=1}^j a_k x^k)] x^j = 0 \end{cases} \quad (5.8)$$

To obtain the numerical values of the coefficients, $j+1$ equations were converted to a matrix form:

$$A = \begin{bmatrix} n & \sum x_i & \sum x_i^2 & \dots & \sum x_i^j \\ \sum x_i & \sum x_i^2 & \sum x_i^3 & \dots & \sum x_i^{j+1} \\ \sum x_i^2 & \sum x_i^3 & \sum x_i^4 & \dots & \sum x_i^{j+2} \\ \vdots & \vdots & \vdots & \ddots & \vdots \\ \sum x_i^j & \sum x_i^{j+1} & \sum x_i^{j+2} & \dots & \sum x_i^{j+j} \end{bmatrix}, X = \begin{bmatrix} a_0 \\ a_1 \\ a_2 \\ \vdots \\ a_j \end{bmatrix}, B = \begin{bmatrix} \sum y_i \\ \sum (x_i y_i) \\ \sum (x_i^2 y_i) \\ \vdots \\ \sum (x_i^j y_i) \end{bmatrix} \quad (5.9)$$

where n – the number of waveforms in the experiment;

j – polynomial order.

To find the coefficients of the polynomial approximation, the formula is used:

$$X = A^{-1}B \quad (5.10.)$$

where X – vector of solutions.

The picture of acoustic emission events in the experiment is formed of two types: AE event with the frequency of the maximum spectral power density within the range from 31 kHz to 38 kHz, and the events with the frequencies of 96 kHz to 103 kHz.

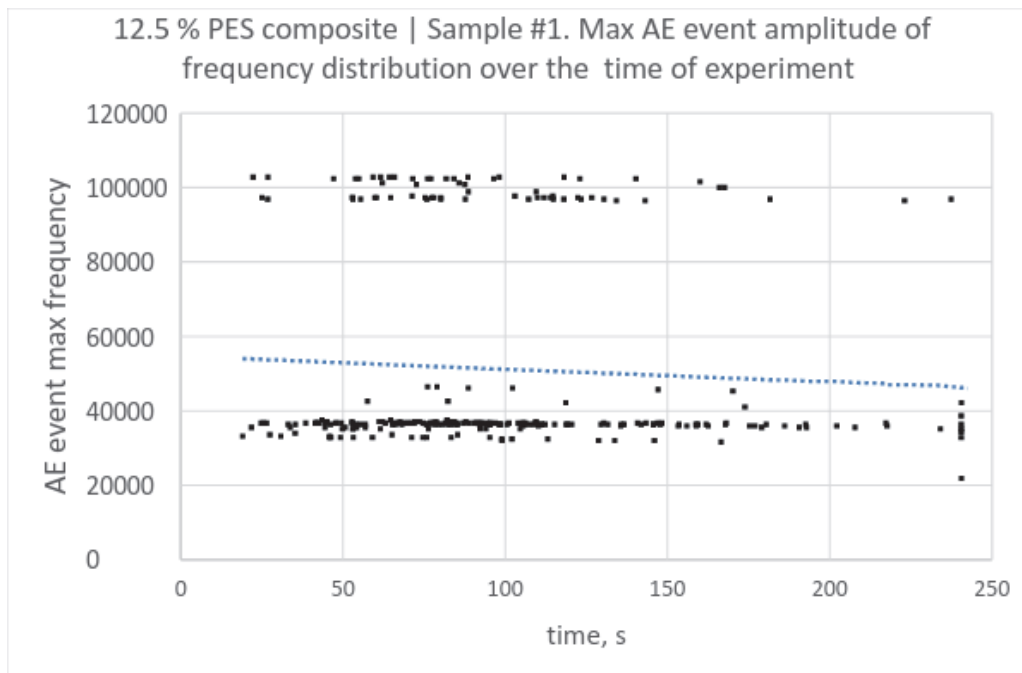


Fig. 5.4. Maximum frequency plot and function approximation in the first experiment with 12.5 % PES concentration ($j = 5$).

On the approximation function graph (Fig. 5.4), the same pattern of the changes in the AE frequency is observed for the values of j from 4 to 6 inclusive. Throughout all the experiment, the frequency generally decreases for the full group of high and low frequencies, as well as separately for both groups. At the same time, after the occurrence of each of the two α -criteria, the way of the change in frequency is changing itself. After the onset of α_1 , the fit-function of a monotonically decreasing becomes a monotonically increasing. The values of the frequency of AE events reach their maximum values. Then, after the registration of the new package of active emission corresponding to α_2 , the fit-function again begins to decrease monotonically and reaches a minimum value just before the sample breaks. At the end of the experiment, it is already at the σ yield point when the sample is approaching to a break, and the last time there is a short-term increase in frequency.

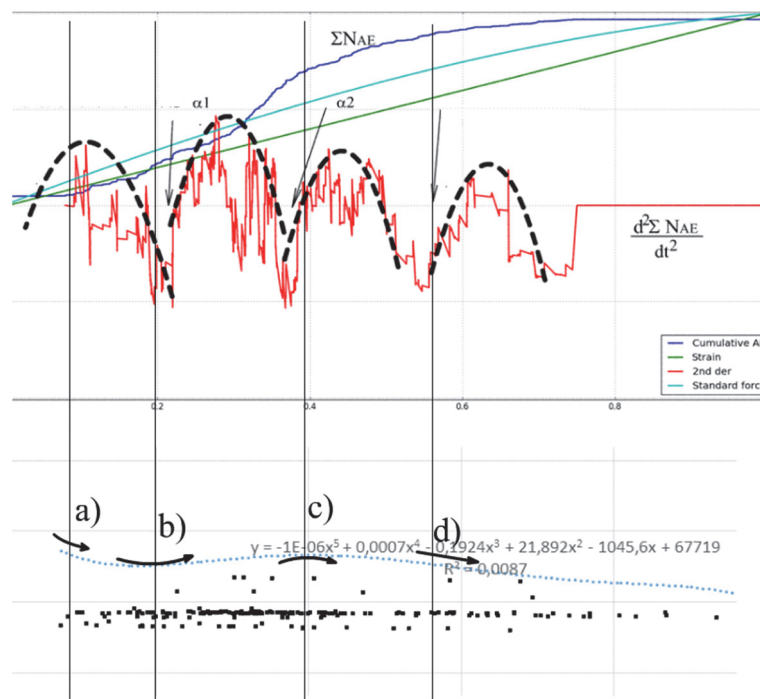


Fig. 5.5. Scheme of compliance of the 2nd derivative of total AE and the dynamics of the approximating function of the maximum frequency in the 1st experiment with the content of 12.5 % PES.

Thus, four distinct phase change dynamics of AE are illustrated in Fig. 5.5. Each stage is characterized by a unique, peculiar only to itself, combination of two parameters: the dynamics of the 2nd derivative of the total AE, and the dynamics of the maximum power spectral density. All phases observed are summarized in Table 5.1.

Table 5.1
The relationship of dynamics of parameters of AE signals and the stage of destruction

No. of situation	Characteristics of the stage	Behavior of the fit-functions of the frequency of maximum spectral power density	The behavior of the 2nd derivative of the cumulative AE count	Stage marking
1	Start of AE accumulation	Decreases with flattening	Reducing changes to growth	a)
2	α_1	Lower extreme. Reduction replaced by growth	Reducing changes to growth	b)
3	α_2	Upper extreme. Growth replaced by reduction	Reducing changes to growth	c)
4	Ultimate strength achievement	Uniform reduction	Reducing changes to growth	d)
5	The area on which 2nd derivative has a local minimum, but the change in the form of cracking does not occur. Without the use of a frequency setting section, it can be mistakenly identified as an event of the groups 1–4.	Growth	Reducing changes to growth	Interval between (b) and (c)
6	All other intervals	Change occurs	Function dynamics does not show the change in the decrease of growth	All other intermediate intervals

In addition to the four stages of the composite sample destruction, which are associated with an obvious decrease variation in the second derivative of AE on the total growth in most of the experiments with the samples, was also a detected phase, which may be erroneously classified as a type of change in the fracture. This step is the section (b)–(c) in Fig. 5.5. In order to eliminate the possibility of misclassification of this step, a frequency parameter was used.

It was concluded that **cumulative-AE-criterion (α -criterion) is a parameter related to the dynamics of change in frequency**. Its use suggests the following approach: starting from an arbitrary point in the time immediately after the release of acoustic emission having the typical 2nd derivative pattern change, it is necessary to refer to the change in the frequency of AE events. By the nature of the changes in the function approximation, the maximum frequency of AE signals can be determined in the stage of failure during testing.

In order to create a two-feature classification training set, the features listed in Table 5.2 were quantified using ordinal numbers.

Table 5.2. Quantified classification pattern representation of AE features

Class	Classification feature		Structural health assessment of composite material during tensile test				
	Feature 1: Cumulative smoothed AE 2nd der. sign (code 1..2)	Feature 2: Peak frequency dynamics (code 1..6)	Relative destruction load estimation [0 to 100% of breakdown load]				
Destruction mechanism			For PES 0 %	For PES 5 %	For PES 7.5 %	For PES 10.0 %	For PES 12.5 %
1	1	1	<5 %	<20 %	<15 %	<10 %	<18 %
2	1	2	≈5 %	≈20 %	≈15%	≈10 %	≈18 %
3	1	3	≈85 %	≈55 %	≈45%	≈38 %	≈40 %
4	1	4	>85 %	>55 %	>45 %	>38 %	>40 %
5	1	5	5 %..85 %	20 %..55 %	15 %..45 %	10 %..38 %	20 %..55 %
6	2	1...5	Not defined. Resume AE-recording for identification.				

Number of PES samples: 30. Number of classification samples: 30×6 classes = 180. A classification sample is one of [1...6] stages of epoxy sample destruction.

5.8 Method verification

The process of method verification was conducted the same as in (3.3).

Number of positive samples (classes 1..5) (P): 194.

Number of negative samples (6th class) (N): 41.

Number of true positive (TP): **180**.

Number of true negative (TN): **30**.

Number of false positive (FP): 14.

Number of false negative (FN): 11.

False positive rate (type I error): $FP/(FP+TN) = 31 \%$.

False negative rate (type II error): $FN/(TP+FN) = 5 \%$.

Classification accuracy: $(TP+TN)/(TP+FP+FN+TN) = 89 \%$.

Table 5.3. Summary of the application of feature classification

No. of objects	Description of the object of assessment	Software processing of the waveform	Classification features	Number of classes
30	PES-filled epoxy composite	Yes Converting to relative coordinates Spectral analysis	1. Peak frequency 2. λ -criterion second derivative	6: corresponding to epoxy composite tensile test program

The summary of the features used in the above-described method is shown in Table 5.3. Note that the amount of 11 false negative classifications does not mean that at some point, the stage of destruction was classified in favor of an unnoticed approach to the point of destruction. This only means that in 11 cases, the method has indicated that a specialist should keep record of AE data. Taking a longer sample (10 to 20 seconds of recording AE), the classification gave a correct result.

Summary of Chapter 5

The developed software has helped to define the parameters of the relationship dynamics of the appearance of the AE signals and the dynamics of the frequency pattern of signals in the composite samples. This conclusion requires further inspection for other groups of materials: metals, alloys, and other concrete used in transport facilities. Simultaneous use of the criterion of the second derivative and the criterion of the change of the maximum frequency of events can help identify the phase of

the sample destruction, starting from an arbitrary recording location. At the same time, identification interval is a minor. It is sufficient to have AE of several tens of events to observe the features characterizing the stage of the destruction.

Additional experiments on the simultaneous recording of data have also been supplied with the help of various AE computers (*Lel*, *PocketAE*, and *Pac3000*). The data is then combined with the help of the developed program, and the possibility of their sharing has been ascertained. At the same time, it was necessary to make settings in the program, because different manufacturers of AE computers use different numbers of recording format, the form header files, and other proprietary information. That points to the relevance of the debate on the possibility of developing and implementing an industry standard of AE files export.

It was shown that an essential step towards the adoption α -parameter as technical condition assessment criterion of engineering structures and their objects is the parameter binding with other AE features. Developing this and other assessment criteria is extremely important, because it leads to the creation of effective AE testing methods, usable with technical personnel of enterprises that provide transport networks maintenance. The prospective and robust approach for that is AE patternization and feature classification.

CONCLUSIONS

1. An analysis of the traditional methods of nondestructive testing and AE methods was carried out. The analysis revealed the advantages of using acoustic emission methods. AE methods provide a reliable, holistic approach to assessing the technical condition of objects. The informative value of AE signals is determined by a set of parameters: dynamic, spectral, and others. Based on a critical analysis of the current state of AE control, it is concluded that during the operation of the facilities, crack detection methods are important for monitoring the state of objects, but are often difficult to apply. There is a need to develop and improve the ways to interpret dynamic AE criteria, as well as to use other parameters that carry information about the mechanism of destruction.
2. The mechanisms of destruction for the following land transport facilities were investigated: the Kegums HPP bridge, the frames of the locomotive carriages, and the reinforced concrete sleepers. For the bridge span, the mechanism of the propagation of the AE signal through the damaged-by-corrosion and “healthy” joints was determined. The absence of dangerous structural defects was ascertained. A computer program for determining the similarity of two AE patterns was developed. In the fatigue tests of the locomotive carriage, the possibility of using a dynamic test criterion was confirmed. A method has been proposed and successfully approved, which involves the gradual introduction of concentrators into the construction of the locomotive bogie frame, which saves time in the process of recording the reference object’s AE. In fatigue tests of reinforced concrete sleepers, the dynamic mechanism of the appearance of AE signals at various stages of destruction was studied. The result is also the basis for applying the dynamic criterion of AE as an indicator for such modern materials as polymer composites. In the process of testing the sleepers, the graph of cumulative AE revealed the phenomenon of a “plateau” between the series of the loading of the object. This phenomenon allows drawing a conclusion about the manifestation of the effect of “healing” in concrete under the action of tightening loads of reinforcement.
3. The AE criteria for the tensile tests of PES-filled composites were determined. A method for identifying the fracture stage was developed, which uses the change in the frequency parameter of the maximum spectral density of the AE signals. The relationship between this parameter and the behavior of the dynamic AE criterion was discovered. Based on the results obtained, it was stated that the simultaneous application of the spectral parameter and the intensity parameter of the AE makes it possible to exclude the possibility of erroneous identification of one of the stages of failure.
4. The analysis of the spectral and dynamic properties of AE signals was carried out, and the character of changes in their spectral properties was revealed. A mathematical method for identifying the stage of material destruction was developed. To interpret the dynamic AE criterion, the method of numerical differentiation of the curve of the total AE with a 6 % smoothing parameter was

proposed and applied. The above-mentioned approach reduced the ambiguity of the interpretation of the dynamic parameter. Applying this approach, the intensity parameter of the AE and the spectral parameter were analyzed. As a result, an 89 % accuracy was obtained in determining the fracture stage in the tensile tests of composites.

5. The methodology of the multicriteria AE testing of ground transport facilities was developed to assess the technical condition during operation. Two AE parameters were used to test the bridge span at the Kegums HPP: the average intensity of the AE series, and the duration of the time intervals between the active series of AE. For locomotive carriages, two parameters were used: the slope angle of the cumulative AE plot, and the intensity parameter of the AE. To test the concrete sleepers, three AE parameters were determined: the duration of the “plateau”, the number of cycles between the end of the “plateau” and the onset of the dynamic criterion, and the tangent of the angle of the dynamic AE criterion (α -criterion). For sleepers, as for experimentally tested same-type objects in plural, the accuracy of the method was determined. It was estimated as 90.4 %. The developed method allows detecting the presence of a defect in the object in a relatively short time and with sufficient reliability.

6. Based on the received spectral and dynamic characteristics of AE signals, a software was developed that implements the functions described in the work. The first module allows classifying various AE parameters. The second module allows analyzing the behavior of the dynamic AE parameter in relative coordinates, which makes it possible to compare the results of the experiments of different duration. The third module allows determining the behavior of the parameter of the maximum spectral density and, thus, to use this parameter for the multiparameter AE classification of the stages of damage. The functionality of all modules in the process of analyzing the data of the investigated objects was tested. The sufficient functionality of the software and its compliance with the tasks being solved was shown.

BIBLIOGRAPHY

1. Ai, Y. A., Sun, C. A., Que, H. B. & Zhang, W. A., 2015. Investigation of material performance degradation for high-strength aluminum alloy using acoustic emission method. *Metals*, 13 February, 5(1), pp. 228–238.
2. Amini, A., Entezami, M. & Papaalias, M., 2016. Onboard detection of railway axle bearing defects using envelope analysis of high frequency acoustic emission signals. *Case Studies in Nondestructive Testing and Evaluation*, November, Volume 6, pp. 8–16.
3. Baifeng, J. I. & Weilian, Q. U., 2008. The research of acoustic emission techniques for non destructive testing and health monitoring on civil engineering structures. s.l., CMD, pp. 782–785.
4. Baksi, S. & Biswas, S., 2009. *Composites in Transportation – Indian Scenario*. [Online] Available at: http://tifac.org.in/index.php?option=com_content&view=article&id=564:composites-in-transportation-indian-scenario&catid=85:publications&Itemid=952
5. Banov, M. D., Koniaev, E. A. & Troyenkin, D. A., 1982. The defectoscopy of fatigue strength of gas turbine blades using method of Acoustic Emission. *Defectoscopy*, Volume 8, pp. 26–28.
6. Doroshko, S. & Banov, M., 2008. *Acoustic emission testing of aircraft constructions*. Universidad de Sun Buenaventura, Volume 14, pp. 5–13.
7. European Commission, 2012. *Priority projects*. [Online] Available at: http://ec.europa.eu/transport/themes/infrastructure/ten-t-policy/priority-projects_en [Accessed on 28 February 2017].
8. Fedorus W., Manalo A., Thiru A., Van Erp G., 2014. 23rd Australian Conference on the Mechanics of Structures and Materials (ACMSM23), Design of epoxy resin based polymer concrete matrix for composite railway sleeper, p. 137.
9. Ge, R. D., Yu, A. P. & Lu, H. B., 2011. The setting of Acoustic Emission detecting parameters in running of steel structured. s.l., MACE, pp. 3696–3699.

10. Hellier, C., 2003. Handbook of nondestructive evaluation. s.l.: McGraw Hill.
11. Jiang, A. L., Zhao, Y. H. & Zhang, L. W., 2008. Experimental study of acoustic emission characteristics of underwater concrete structures. s.l., SPAWDA, pp. 252–257.
12. Marchevsky, M. et al., 2016. Localization of Quenches and Mechanical Disturbances in the Mu2e Transport Solenoid Prototype Using Acoustic Emission Technique. IEEE Transactions on Applied Superconductivity, 26(4).
13. Nesterov, E. I., Yegorov, A. T., Perfilov, A. A. & Gudkov, A. V., 1988. The Industry Directory of Locomotives in USSR. Locomotive carriages. Moscow: s.n.
14. Kaewkongka, T., 2016. A train bearing fault detection and diagnosis using acoustic emission. Engineering Solid Mechanics, 4(2), pp. 63–68.
15. Kaiser, J., 1950. Untersuchung über das Auftreten von Geräuschen beim Zugversuch. München: Fakultät für Maschinenwesen und Elektrotechnik der Technischen Universität.
16. Permal Wallace Pvt. Ltd, n.d. FRP Composite Sleepers for Application on Rail Tracks. [Online] Available at: http://www.powershow.com/view1/8efe0-ZDc1Z/FRP_Composite_Sleepers_for_Application_on_Rail_Tracks_powerpoint_ppt_presentation [Accessed on 28 February 2017].
17. Powers, D. M. W., 2011. Evaluation: From Precision, Recall and F-Measure to ROC, Informedness, Markedness & Correlation. Journal of Machine Learning Technologies, 2(1), pp. 37–63.
18. RGS Europa, 2014. Polyurethane Baydur® 60. [Online] Available at: <http://www.rgseuropa.it/en/materials/polyurethane/polyurethane-baydur-60/> [Accessed on 28 February 2017].
19. Swit, G., 2009. Diagnostics of prestressed concrete structures by means of acoustic emission. s.l., ICRMS, pp. 958–962.
20. Urbahs, A. et al., 2010. Acoustic Emission Diagnostics of Fatigue Crack Development during Undercarriage Bench Testing. Kaunas, Kaunas University of Technology, pp. 450–454.
21. Urbahs, A. et al., 2013. Konstruciju skrūvju un kniežu savienojumu kombinētā akustiskās emisijas un ultraskaņas kontroles metode. Latvia, Patent No. G01N29/14.
22. Vallen, H., 2002. AE Testing. Fundamentals, Equipment, Applications. Munich: Vallen-Systeme GmbH.
23. Webb, A. R. & Copsy, K. D., 2011. Statistical Pattern Recognition. 3rd ed. Chichester: Wiley.
24. Ying, S. L., Bo, L. Y. & Ge, L. L., 2012. Comparison of Magnetic Flux Leakage (MFL) and Acoustic Emission (AE) techniques in corrosion inspection for pressure pipelines. s.l., s.n., pp. 5375–5378.
25. Zhang, X. et al., 2015. An investigation on rail health monitoring using acoustic emission technique by tensile test. Pisa, s.n.